Sub-zero soil CO_2 respiration in biostimulated hydrocarbon-contaminated cold-climate soil can be linked to the soil-freezing characteristic curve

Tasnim Nayeema†, Aslan Hwanhwi Lee†, Amy Richter‡, Kelvin Tsun Wai Ng‡, Wonjae Chang†*

*__Corresponding author__: Wonjae Chang,
E-mail: wonjae.chang@usask.ca
Phone: +1-306-966-5373

Affiliation
†Department of Civil, Geological, and Environmental Engineering, College of Engineering
University of Saskatchewan, Saskatoon, Saskatchewan, Canada
57 Campus Drive, Engineering Building, Saskatoon, Saskatchewan, S7N 5A9, Canada

‡ Faculty of Engineering and Applied Science, Environmental Systems Engineering
University of Regina, Regina, Saskatchewan, Canada
3737 Wascana Parkway, Regina, SK, S4S 0A2

Graphical Abstract

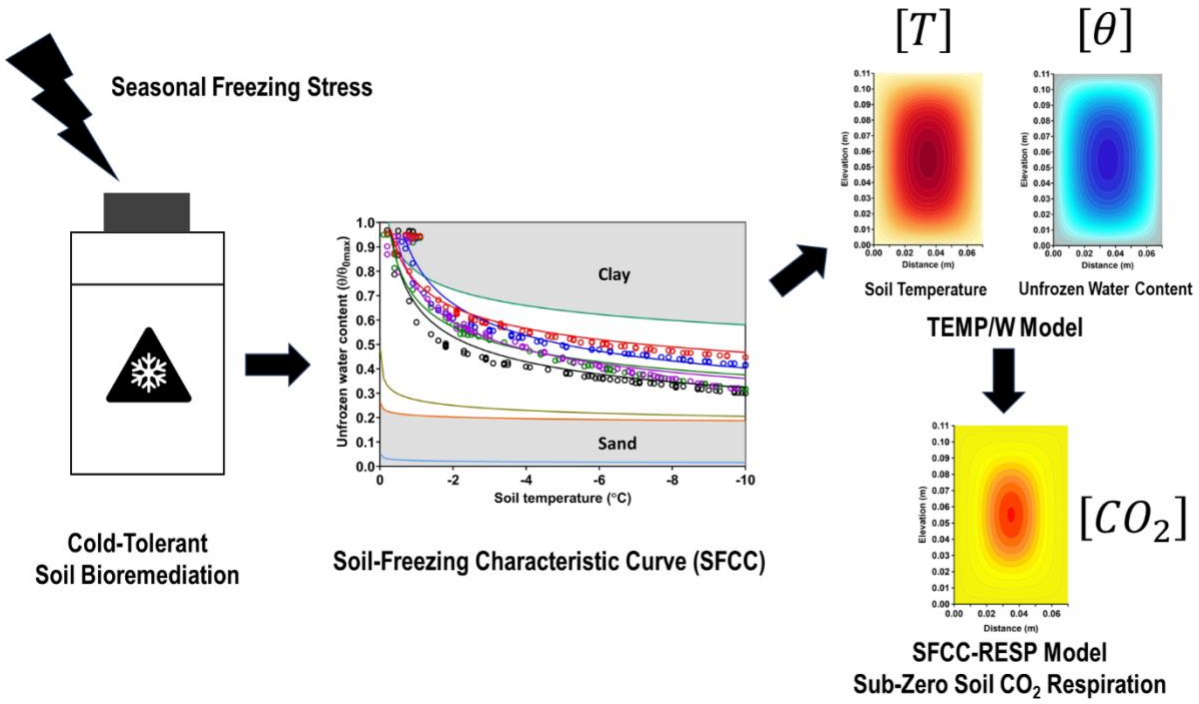

Abstract

Extending unfrozen water availability is critical for stress-tolerant bioremediation of contaminated soils in cold climates. This study employs the soil-freezing characteristic curves (SFCCs) of biostimulated, hydrocarbon-contaminated cold-climate soils to efficiently address the coupled effects of unfrozen water retention and freezing soil temperature on sub-zero soil respiration activity. Freezing-induced soil respiration experiments were conducted under the site-relevant freezing regime, programmed from 4 to -10 °C at a seasonal soil freezing rate of -1 °C/day. The effects of unfrozen water retention on extending soil respiration activity emerged at the onset of soil freezing. The unfrozen water effect became significant below 0 °C (correlation r = 0.83–0.94) and comparable to the temperature effect (correlation r = 0.82–0.90), successfully demonstrating the coupled effects on sub-zero respiration activity. Soil CO_2 respiration modelling based on the temperature dependency only (Arrhenius and Q_{10} models) did not accurately describe sub-zero respiration activity associated with increased unfrozen water retention in treated contaminated soils. The shifted SFCCs of the treated soils, expressed as a function of soil temperature (T) and unfrozen water content (θ), served as a key framework for efficiently developing the sub-zero respiration model (SFCC-RESP). The developed SFCC-RESP model closely approximated the changes in soil respiration rates influenced by T and θ in the treated soils (R^2 = 0.94–0.98) and described the abrupt decrease and subsequent stabilization in CO_2 production during the transition to the deeply frozen soil phase. The SFCC-RESP model integrated with soil thermal models (TEMP/W) can be used to produce spatial distributions of T, θ, and CO_2 production in the treated soil matrix, providing a tool to approximate the abundance of unfrozen habitable niches when developing cold-tolerant bioremediation strategies.

Keyword

Sub-zero soil respiration; Contaminated soils; Soil-freezing characteristic curve; Unfrozen water content; Bioremediation; Cold climates

1. Introduction

For many decades, petroleum hydrocarbons have been frequently identified as organic contaminants in cold-climate soils, including polar and sub-polar soils, while industrial activities have continued to expand and intensify (Aislabie et al. 2006, Chang et al. 2011a, FCSI 2023, Kim et al. 2021, Margesin & Schinner 2001, Miri et al. 2019, Snape et al. 2008). In previous studies and applications, indigenous cold-adapted, hydrocarbon-degrading bacteria have often been shown to be abundant in field-aged, petroleum hydrocarbon-contaminated soils, and can be stimulated by supplying inorganic nutrients (e.g., nitrogen) and solid mineral amendments (e.g., zeolites and biochar) to site soils (Aislabie et al. 2006, Braddock et al. 1997, Chang et al. 2011a, Coulon et al. 2004, Karppinen et al. 2017a, Kim et al. 2021, Margesin 2000, Martínez Álvarez et al. 2022, McCarthy et al. 2004, Walworth et al. 2001, Whyte et al. 2001). Enhancing hydrocarbon biodegradation in petroleum-contaminated soils was feasible for diverse cold-climate site soils of varying types (clayey and sandy soils) and hydrocarbon contaminants (semi- and non-volatile hydrocarbons) at the *in situ* or simulated temperatures of summer (e.g., ~4 to 10 °C), and even at sub-zero temperatures under *in situ* and simulated seasonal freeze-thaw conditions (e.g., -10 to 4 °C) (Børresen et al. 2007, Chang et al. 2010, Chang et al. 2011a, Eriksson et al. 2001, Gomez & Sartaj 2013, Karppinen et al. 2019, Kim et al. 2018, 2021, Martínez Álvarez et al. 2020, Martínez Álvarez et al. 2017, Paudyn et al. 2008).

Soil CO_2 gas, a final mineralization product of hydrocarbon biodegradation, is regarded as a useful *in situ* indicator of soil respiration activity for tracking microbial enhancement and bioremediation progress in cold region sites (Aspray et al. 2008, Chang & Ghoshal 2014, Gomez & Sartaj 2013, Kim et al. 2018, Mair et al. 2013, Rike et al. 2003, Rike et al. 2005). Soil respiration activity is often monitored by the rates of CO_2 production and/or O_2 consumption, which are influenced by several abiotic and biotic factors (Elberling & Brandt 2003).

Temperature is considered the key driver in regulating soil respiration activity (Davidson et al. 2006, Lellei-Kovács et al. 2016), and the temperature dependency of soil respiration has been extensively explored through Arrhenius-based models and the Q_{10} relationships (Lloyd & Taylor 1994, Moinet et al. 2018, Qi et al. 2002). Other factors such as substrate type, organic matter, substrate availability, water content (or unfrozen water availability), microbial biomass, microbial community, and oxygen supply also have an influence on soil respiration activity. These factors have been considered more recently for improving soil respiration models under various *in situ* environmental conditions, beyond the temperature dependency of soil respiration.

However, the soil respiration models available are not adapted to express soil respiration activity under the seasonal freeze-thaw conditions in contaminated soils that have received a biostimulation treatment, with the exception of the URESP model reported by Kim and Chang, (2019). The URESP model is based on the modified, substrate-dependent Michaelis-Menten expression (Kim & Chang 2019). Unfrozen water carrying dissolved substrates is a fundamental requirement for the survival and sub-zero metabolic activity of cold-adapted microorganisms in frozen environments (Deming 2002, Öquist et al. 2009, Panikov et al. 2006, Rivkina et al. 2000, Tilston et al. 2010). Unfrozen water can be detected in freezing and frozen contaminated soils treated with liquid nutrients and/or solid soil amendments (e.g., zeolites and biochars), as observed in microcosm- and pilot-scale biodegradation experiments carried out at sub-zero temperatures (Chang et al. 2011a, Karppinen et al. 2017b, Kim et al. 2021, Siciliano et al. 2008). In an outdoor pilot-scale biopile experiment carried out in the winter in Saskatchewan, Canada, unfrozen water content was detected in seasonally freezing petroleum-hydrocarbon-contaminated soils that received liquid nutrients and humate, which was associated with the significant biodegradation of non-volatile hydrocarbons that occurred in the winter season (Kim et al. 2018).

Unfrozen water retention in freezing contaminated soils can be manipulated by treating soils with liquid nutrient and solid zeolite amendments. Respectively, these amendments elevate nutrient solutes and increase soil surface area, which also stimulate indigenous hydrocarbon-degrading bacteria (Kim et al. 2021). Unfrozen water retention in frozen soils has been explained by soil water potential (osmotic and matric potentials), which states that concentrated solutes in unfrozen water influence the osmotic potential of the water (Drotz et al. 2009, Konrad & McCammon 1990, Ma et al. 2017, Wen et al. 2012). Soil properties such as surface area, particle size, pore size, pore networks, and soil organic matter influence matric potential, which regulates unfrozen water availability (Drotz et al. 2009, Wen et al. 2012). Increased unfrozen water retention in successfully biostimulated soils has been directly related to meaningful biodegradation in freezing hydrocarbon-contaminated soils, as confirmed by observed shifts in the microbial communities in the treated and untreated hydrocarbon-contaminated soils undergoing freezing (Chang et al. 2011a, Karppinen et al. 2017b, Kim et al. 2018, 2021). Therefore, under freezing conditions, the temperature effect alone cannot account for sub-zero microbial respiration activity in biologically active contaminated soils and organic-rich pristine soils in cold environments (Byun et al. 2021, Nikrad et al. 2016, Rike et al. 2005).

Soil respiration models for extended biological activity in stimulated contaminated soils under seasonal freeze-thaw have not been extensively proposed, although unfrozen water retention in soil during freezing has been represented. Unfrozen water retention in freezing hydrocarbon-contaminated soils treated for bioremediation can be represented by the soil-freezing characteristics (SFCC) (Kim et al. 2021). Using the SFCC equation expressed as a function of soil temperature (T) and unfrozen water content (θ) appears to be a promising approach in addressing the coupled effects of soil temperature and unfrozen water on extended

soil respiration activity in treated contaminated soils during seasonal freezing. The SFCCs of various soils in cold regions (e.g., sandy and clayey soils) have been well reproduced and the SFCC is used in the literature as an engineering soil property and index for seasonally frozen soils (Andersland & Ladanyi 2003, Anderson et al. 1973, Devoie et al. 2022, Farouki 1981). Yet, the feasibility of linking SFCCs to soil respiration modelling in contaminated soils in cold climates has not been suggested.

Therefore, the study aims to incorporate the soil freezing characteristics into soil respiration modelling using the experimental and simulated SFCCs of biologically enhanced hydrocarbon-contaminated cold-climate soils subjected to seasonal freezing stress, and, thus, to develop a SFCC-based soil respiration model that accounts for sub-zero respiration activity in seasonally freezing biostimulated contaminated soils. Briefly, to produce experimental SFCCs and soil respiration activity data (CO_2 production rate), induced-freezing soil microcosm experiments were conducted, during which the soil temperatures decreased from 4 to -10 °C at an average seasonal soil freezing rate of -1 °C/day using field-aged, hydrocarbon-contaminated, cold-climate soils treated with nutrients, zeolite and porous carbon for biostimulation. Then, the temperature dependency of soil respiration activity during freezing in the biostimulated contaminated soils was evaluated using the soil respiration models based only on the temperature effect (Arrhenius and Q_{10} models). Using the experimental SFCCs of the treated soils, a newly proposed soil respiration model called the SFCC-RESP model was then developed for coupling soil temperature and unfrozen water effects on the extension of soil respiration in seasonally freezing contaminated soils treated for bioremediation. A numerical soil thermal modelling tool (TEMP/W model) produced high-throughput data for the simulated SFCCs of the treated soils. The SFCC-RESP model combined with the TEMP/W model then produced the spatial

distributions of soil temperature, unfrozen water content and CO_2 production rates throughout the soil phase transition from partially to deeply frozen, which can be an intuitive tool for approximating sub-zero soil respiration activity and the distribution of unfrozen water niches required for developing cold-tolerant bioremediation strategies for cold impacted site soils that are less accessible, more environmentally sensitive, and ecologically fragile.

2. Materials and methods

2.1. Contaminated soil

The contaminated soil used for this study was shipped from an outdoor soil remediation facility in Saskatoon (PINTER and Associates Ltd.). Table 1 summarizes the physical, chemical and microbial properties of the petroleum hydrocarbon-contaminated soil obtained from a cold site. The site soil comprises 6% gravel, 5% coarse sand, 14% medium sand, 44% fine sand, 16% silt and 11% clay, and it is classified as poorly graded sand with gravel using the Unified Soil Classification System (USCS). Based on the United States Department of Agriculture (USDA) method, the soil texture is classified as a sandy loam (Table 1). The soil used for this study contains a significant amount of fine-grained silt and clay particles, over 20-30% by weight, based on both USCS and USDA methods. This finer soil fraction is much larger than in the site soil (sand) used for the previous soil respiration modelling study (URESP model) extended to sub-zero respiration activity, which contained only 2% silt and clay (Kim & Chang 2019). The non-volatile hydrocarbon fraction, defined as > C16 to C34 (F3 hydrocarbons), is the dominant hydrocarbon fraction and is present in the range of 1200 to 9000 mg/kg (Table 1). The concentration of the semi-volatile hydrocarbon fraction (F2 hydrocarbons) ranges from as low as non-detectable to 2000 mg/kg. Inorganic Nitrogen (N) is largely deficient in the site soil; however, phosphorus (P)

is not limited. Viable indigenous bacteria capable of degrading organic carbon and hydrocarbons in the diesel range (F2 and F3 hydrocarbons) are abundant, with populations broadly ranging from 2.5×10^4 to 4×10^7 CFU/g from 4 to 22 °C. The pH of the site soil was measured at 7.6. The significant number of viable indigenous heterotrophs and hydrocarbon-degrading bacteria enumerated in the site soil is indicative of biostimulation potential, as similarly observed in previous bioremediation studies for petroleum-contaminated, cold-climate soils (Aislabie et al. 2004, Chang et al. 2011b, Kim et al. 2021).

Table 1

2.2. Biostimulation amendments

2.2.1. Liquid nutrient amendment

The preliminary characterization of this site soil indicated the rapid growth of heterotrophs at both 10 and 22 °C in the soil amended with inorganic liquid nutrients (20:20:20 N-P-K composed of 20% total N, 20% P_2O_5, 20% K_2O, Plant Prod®) (Nayeema et al., 2023). Preliminary biostimulation feasibility experiments determined that a nutrient dose of 200 mg N/kg using the N-P-K solution was favourable for increasing the population size of viable heterotrophs in the site soils, compared to the lower or higher doses (i.e., 100 mg N/kg and 300 mg N/kg) (Braddock et al. 1997, Chang et al. 2010). In this study, 200 mg N/kg was therefore used for the freezing-induced soil respiration experiment.

2.2.2. Solid mineral amendments

Zeolite is used in this study as a solid mineral amendment (~44 μm) for retaining unfrozen water in the soil subjected to seasonal freezing stress, as suggested in our prior publication (Kim et al. 2021). The zeolite species used is analcime zeolite (ZMM® Canada Minerals Corp, Canada; Table S1). The porous carbon amendment (5000 mg/kg of organic carbon), a product of pyrolysis of pine wood chips (T-carbon; ZMM® Canada Minerals Corp, BC, Canada; Table S1), was used as a porous amendment (up to 16 mm) to provide additional microbial habitats and readily bioavailable carbons. The compositions of the zeolite and carbon amendments are available in the Supplementary Information. Detailed information about the material properties of zeolite and porous carbon is available in Table S1 (Supplementary Information).

2.2.3. Predetermination of zeolite dosage and initial water content

The soil drying process is similar to the soil freezing process in terms of the temporal reduction in water availability. To determine the dosage of zeolite as a source of microbial habitats under water-stressed conditions, a soil drying experiment was conducted at a constant room temperature (22±1° C) to eliminate the interaction between temperature and water availability for microbial survivors. The determined zeolite dosage was applied to the following freezing-induced soil respiration experiments using the field contaminated soils amended with zeolite and a nutrient solution.

Briefly, Ottawa soil microcosms spiked with 0.5% (v/v) diesel and amended with Bushnell Hass (BH) nutrient media were inoculated with *Dietzia maris* strain FTI08 (Genbank accession number: KX344942.1), which was characterized as a halotolerant heterotroph obtained from hypersaline potash mining byproducts (tailings and brine) (Harris 2017). Detailed information about *Dietzia maris* as a halotolerant, hydrocarbon degrader and other halotolerant bacterial communities from potash mining byproducts is available in our prior publications (Chang et al. 2018, Harris et al. 2023). In this setup, diesel is the only carbon source for bacterial growth in the soil system. Ottawa

sand was used as a standard sand (quartz) to isolate the effect of zeolite addition from the effects of any background clay minerals present in natural soils. The initial water content of all soil sets before soil drying was equal and set at 15% (w/w). The prepared sand microcosms were further amended with zeolite (0, 1, 2, 5 and 10% w/w). Control soil microcosms (diesel + Ottawa sand + BH nutrient + *Dietzia maris*, with no zeolite) were prepared as well, and their initial water content was maintained, without soil drying, for comparison with the zeolite-amended soil sets under drying conditions. All experiments were conducted in triplicate. The weight loss (water evaporation) during the soil drying experiment was tracked to estimate the change in water content over time. Soil samples were aseptically collected when no significant change observed in the monitored water content in the soil microcosms subjected to soil drying, and the viable populations of hydrocarbon degraders (*D. maris* strain strain FTI08) were enumerated (CFU; colony forming unit per gram of soil). The zeolite dosage used in the other experiment to determine the initial water content for the freezing-induced respiration was constant (5% w/w), and other factors (bacteria, nutrient concentration, diesel and soil matrix) were the same as those above. However, the initial water content was variable from 0 to 12.5, 15, 17.5 and 20% (w/w).

2.3. Seasonal freezing-induced respiration experiment

2.3.1. Soil treatment

Prior to the freezing-induced respiration experiments, five sets of treatment microcosms were aseptically prepared using the site soil based on the predetermined doses of the nutrient, zeolite and carbon amendments, as follows: (1) *200N + 2%Z,* (2) *200N + 2%Z + 1%TC,* (3) *200N + 2%Z + 2%TC,* (4) *200N + 2%Z + 5%TC,* and (5) *Untreated (control)*. The first treatment microcosm above (*200N + 2%Z*) received the N-P-K and zeolite amendments at the predetermined doses (200

mg N/kg and 2% w/w zeolite) but did not receive the carbon amendment (*TC*). The other three treatment microcosm sets received the nutrients and zeolite at the same doses, in combination with varying carbon amendments (1, 2 or 5% w/w). The final untreated (control) set is the soil microcosm set that received no amendments. The water content of the treated and untreated soils was adjusted to 15% (w/w) of the initial gravimetric water content.

2.3.2. Soil microcosm setup for the freezing-induced respiration experiments

About 100 g of the treated and untreated (control) site soils above were aseptically placed into customized 500-mL glass jars, each equipped with a soil gas sampling port and a valve to measure soil respiration without soil disturbance (respiration microcosms). Separately, about 500 g of the same treated and untreated soils were placed in sterilized amber jars to simultaneously monitor soil temperature and unfrozen water content (monitoring microcosm). All microcosms were duplicated. The microcosms were then subjected to a representative seasonal freezing stress of -1 °C/day using a temperature-programmable incubator (MIR-254-PA, Panasonic, Japan), as suggested in the prior bioremediation studies conducted under *in situ* and simulated seasonal freezing conditions (Kim et al., 2021, 2018). The freezing-induced experiment was run for 15 days, during which the temperature was programmed to decrease from 4 to -10°C at the average seasonal soil freezing rate (Figure 1).

Figure 1.

2.3.3. Monitoring

Soil CO_2 production rates in the treated and untreated respiration microcosms under the freezing condition were measured at 24-hour intervals by directly connecting a portable gas monitor to the gas sampling ports fitted to each of the microcosms, as explained above. The gas monitor was equipped with CO_2 infrared sensors with a resolution of 0.01% (v/v) and a low working temperature of -20 °C (MX6i multi-gas detectors, Industrial Scientific, Pittsburgh, USA). The respiration microcosms provided the soil respiration data (CO_2 production rate) for the treated and untreated site soils subjected to seasonal freezing.

A probe was inserted into each of the monitoring microcosms to continuously monitor changes in soil temperature and unfrozen water content in the treated and untreated soils under the simulated freezing conditions. The monitoring probes consist of a thermistor for soil temperature and a frequency domain reflectometry (FDR) sensor for volumetric water content (5TM VWC + Temp; EM50, Decagon Devices, Decagon Devices, Pullman, USA), as similarly described elsewhere in the relevant studies (Kim et al. 2018, 2021, Yoshikawa & Overduin 2005). The probes embedded in the monitoring jars were connected to two data loggers (EM50, Decagon Devices, Decagon Devices, Pullman, USA) placed in the temperature-programmable incubator (Figure 1). The monitoring program for the soil microcosms subjected to seasonal freezing temperatures was set to transfer the collected data to the data logger every 2 hours. The monitoring microcosms provided the measured soil temperature and volumetric unfrozen water content data needed to produce the experimental soil-freezing characteristic curves (SFCC) for the treated and untreated site soils.

2.4. Modelling study

2.4.1. Overall workflow of the modelling study

As shown in Figure 2, this modelling study was divided into five steps: (1) Experimental data acquisition, (2) Evaluation, (3) Model development, (4) Sensitivity analysis, and (5) Application. In step (1), the experimentally measured datasets for soil temperature (T), unfrozen water (θ), soil CO_2 gas production rate, and SFCCs were obtained from the microcosm-scale soil freezing experiment for data acquisition, in which the treated and untreated petroleum hydrocarbon-contaminated field soils were subjected to seasonal freezing conditions (4 to -10 °C). In step (2), the temperature dependency of experimental CO_2 production rates in freezing soils was then evaluated using the conventional Arrhenius and Q_{10}-based models to demonstrate the need to incorporate unfrozen water content into the modelling. In step (3), the new respiration model called the SFCC-RESP model was developed by linking both the measured and simulated SFCCs to Arrhenius-based kinetic respiration modelling to address the coupled effects of temperatures and unfrozen water content on microbial activity in successfully biostimulated contaminated soils during seasonal freezing (*200N + 2%Z + 1%TC*). The experimental SFCC of the treated soil, expressed as a function of T and θ, was used as an input for developing the soil respiration model extended to sub-zero temperatures and predict CO_2 production rates, and the new model was validated by comparing the experimental and computed CO_2 data. In step (4), the sensitivity analysis for the key model variables was conducted for the *200N + 2%Z + 1%TC* microcosms. The resulting SFCCs were then fed into the SFCC-RESP model to generate spatial distributions of T, θ, and CO_2 gas concentrations in the soil microcosm. In step (5), the validated SFCC-RESP model framework with integrated numerical soil thermal modelling (TEMP/W) was then applied to the site soils that received different biostimulation treatments (*200N + 2%Z*, *200N + 2%Z + 2%TC*, and *200N + 2%Z + 5%TC*).

Figure 2.

2.4.2. Temperature-dependent soil respiration models

The Arrhenius equation and Q_{10}-based soil respiration models were employed to evaluate the temperature-dependency of the soil respiration rate between 4 and -10 °C, using non-linear curve-fitting for the experimental data (GraphPad Prism 9.1.2). The general form of the Arrhenius equation is provided below, where *RESP* is the soil respiration rate (mmol CO_2/kg/min), *A* is the Arrhenius coefficient, E_a is the activation energy (J/mol), *R* is the ideal gas constant (8.314 J/K·mol), and *T* is the absolute temperature (K).

$$RESP = Ae^{\left(-\frac{E_a}{RT}\right)} \quad (1)$$

The Q_{10}-based soil respiration modelling is divided into two steps: determining the system-specific Q_{10}-value and computing the temperature-corrected soil respiration rate. The Q_{10} relationship is widely considered in previous soil respiration studies (Davidson et al. 2006, Lloyd & Taylor 1994, Makita et al. 2018, Mundim et al. 2020) and is expressed in Eq. (2), where R_1 and R_2 are the soil respiration rates (mmol CO_2/kg/min) at temperatures T_1 and T_2 (K), respectively.

$$Q_{10} = \left(\frac{R_1}{R_2}\right)^{\frac{10}{T_1 - T_2}} \quad (2)$$

The temperature-corrected respiration rate was computed using Eq. (3), as employed in Davidson et al., (2006), where *RESP* is the temperature-corrected soil respiration rate (mmol CO_2/kg/min),

T is the temperature at any point (°C or K), R_{basal} is the respiration rate at a base point (mmol CO_2/kg/min), and T_{basal} is the corresponding temperature at the base point (°C or K).

$$RESP = R_{basal} \times Q_{10}^{\frac{T-T_{basal}}{10}} \quad (3)$$

The results of the modelling analyses were interpreted using the common statistical parameters: the goodness of fit (R^2), Root Mean Square Error (RMSE), and Mean Absolute Relative Error (MARE).

2.4.3. Development of soil respiration model extended to seasonal freezing conditions

In this study, the experimentally determined SFCCs of the treated soil microcosms were employed to develop the new respiration model. The new model framework was produced by incorporating the common SFCC expression ($\theta = \alpha T^{\beta}$), to the exponential relationship of soil respiration activity (CO_2 data) to freezing temperatures. The coupled effects of freezing temperatures and unfrozen water content were expressed by introducing a product of the temperature and unfrozen water content below 0 °C, denoted as X in Eq. (4), where T is the absolute value of a negative temperature (°C), and θ is the volumetric unfrozen water content (m^3/m^3):

$$X = T \times \theta \quad (4)$$

From Kim et al., (2021) and Andersland & Ladanyi (2003), a simple form of the soil-freezing characteristic curve (SFCC) is expressed with T and θ in Eq. (5), where α and β are fitting constants related to characteristic soil parameters:

$$\theta = \alpha T^{\beta} \quad (5)$$

Substituting Eq. (5) into Eq. (4) produces Eq (6), which can be incorporated into the general form of the exponential decay function, Eq. (7), where $RESP$ is the CO_2-based soil respiration rate (mmol CO_2/kg/min), k is the fitting constant, and r_i and r_p, respectively, are the upper and lower limits in the concentration of CO_2 within the sub-zero temperature regime, which encompasses respiration activity during the soil phase change. X_0 is the product of T_0 and θ_0, as expressed by Eq. (8).

$$X = T \times \theta = T\left(\alpha T^{\beta}\right) = \alpha T^{\beta+1} \quad (6)$$

$$RESP = r_p + \left(r_i - r_p\right)e^{-k(X-X_o)} \quad (7)$$

$$X_o = T_o \times \theta_o \quad (8)$$

The conceptual diagram presented in Figure 3 combines the CO_2 production rate profile and SFCC to represent graphically, in terms of T_o and θ_o, the point at which soil respiration activity, or CO_2 production rate, abruptly drops.

Figure 3.

Eq. (7) can be expressed in terms of T_o and θ_o, as shown in Eq. (9). The SFCC parameters α and β are incorporated into Eq. (10) to produce the SFCC-based respiration model.

$$RESP = r_p + (r_i - r_p)e^{-k(T\theta - T_o\theta_o)} \quad (9)$$

$$RESP = r_p + (r_i - r_p)e^{-k\alpha(T^{(\beta+1)} - T_o^{(\beta+1)})} \quad (10)$$

In this study, Eqs. (7), (9), and (10) are referred to as the SFCC-RESP model that is expressed as a function of temperature (T) and the unfrozen water content (θ) or SFCC parameters (α and β). The results of the SFCC-RESP analysis were validated with the experimental data using the statistical parameters R^2, RMSE and MARE.

2.4.4. SFCC-RESP model with TEMP/W model

The input data for the SFCC-RESP model, measured T and θ (or SFCC parameters), were obtained from the freezing-induced experimental data (described in Section 2.3.3) used to produce the experimental SFCC for each of the four different treated site soils. These experimental SFCCs were transferred to the TEMP/W model to produce the high-throughput datasets for *predicted* T and θ over time in freezing soil. The TEMP/W software is a transient soil thermal numerical model based on the finite element method (FEM) (GEO-SLOPE International Ltd., Calgary, Canada). The use of measured and predicted T and θ for the SFCC-RESP model is presented in Figure 2, describing the overall flowchart of this experimental and modelling study. Using the TEMP/W model, the spatial distributions of T and θ in the treated monitoring microcosms subjected to the average seasonal soil freezing rate of -1 °C/day were predicted over time (2-hour intervals for 11 days of freezing from 0 to -10 °C). Detailed information about the

input data for the TEMP/W soil thermal simulation of freezing contaminated soils treated with nutrients and mineral amendments is presented in the Supplementary Information (Figures S1 to S3, and Table S2), and includes the boundary conditions, input soil thermal parameters, and mesh domains of the microcosms. The predicted T and θ for each element of the microcosm domains were then transferred to the SFCC-RESP model to produce the spatial distribution of predicted CO_2 production rates (respiration) in the treated soils over the freezing period (Supplementary Tables S3 and S4). The time series of predicted CO_2 production rates in the treated soils were validated using the experimental CO_2 data. The spatial distributions of predicted T, θ, and CO_2 production in the freezing and frozen treated soils were demonstrated as T, θ, and CO_2 contour maps using the visualization tool Surfer 13 (Golden Software Inc., Colorado).

3. Results

3.1. Effect of zeolite on microbial survivability under water-stressed conditions

Figure 4(a) presents changes in water content in zeolite-amended or unamended sand inoculated with salt-tolerant hydrocarbon degrader *Dietzia maris* strain FTI08, which were subjected to water scarcity stress, and all microcosm sets experienced drying except the control without drying. Figure 4(b) shows the corresponding surviving numbers of *Dietzia maris* (CFU per g of soil) from the sand under water-stressed conditions. The numbers of microbial survivors in the sands amended with 5% (w/w) zeolite at the various initial water contents, from 12.5% and 20% (w/w), went from 1.28×10^6 to 3.82×10^6 CFU/g, which was similar to the control sand that was not subjected to drying (1.75×10^6 CFU/g). However, the absence of zeolite (*15%WC + 0%Zeo*) significantly reduced the number of microbial survivors by over four orders of magnitude to 3.1×10^2 CFU/g from $>10^6$ CFU/g in the zeolite-amended sands and control sands without drying

(Figure 4(b); one-way ANOVA test and Tukey's multiple comparison test, $p < 0.0001$). As shown in Figure 4(c), the effect of the zeolite amendment on microbial survival in sand subjected to drying was also significant at the constant initial water content of 15% (w/w) (one-way ANOVA test and Tukey's multiple comparison test, $p < 0.0001$). The sand microcosms amended with zeolite in excess of 2% (w/w) showed the significant survival of *Dietzia maris* (1.3–3.3 x 10^6 CFU/g). The number of viable survivors in the sands amended with zeolite in the range of 2% to 10% (w/w) at a constant 15% initial water content (1.7 x 10^6 CFU/g) was equivalent to the populations in the control sands without drying (1.7 x 10^6 CFU/g). The 2% (w/w) zeolite amendment was as effective in supporting microbial survivability as the greater zeolite dosages (5 or 10% w/w) with the same initial water content of 15% (w/w), which provided the rationale for selecting the 2% zeolite dosage and initial water content of 15% for the freezing-induced soil respiration experiments (Figure 4(c)). Overall, the soil-drying experiment suggested that zeolite can be considered a soil amendment for supplying habitats for microbial survival under water-stressed conditions.

Figure 4.

3.2. Freezing-induced soil experiment: Enhanced soil CO_2 respiration

As shown in Figures 5 and 6, soil respiration in all treated contaminated soils, estimated by soil CO_2 production, was higher than in the untreated soils (control) when temperatures were decreased from 4 to -10 °C at the seasonal soil freezing rate of -1 °C/day. Among the treated microcosms, the *200N + 2%Z + 1%TC* microcosms exhibited the highest CO_2 production rates (total 514 mmol CO_2/kg). The *200N + 2%Z + 1%TC* microcosms received all three amendments (nutrients, zeolite, and porous carbon) at moderate levels compared to previous studies of hydrocarbon-contaminated soils in cold climates. The *200N + 2%Z* microcosms amended with nutrients and

zeolite only (without carbon), exhibited the second highest cumulative CO_2 production (total 416 mmol CO_2/kg). The microcosms that received higher porous carbon doses of 2% and 5% (w/w) in combination with nutrients and zeolite (*200N + 2%Z + 2%TC* and *200N + 2%Z + 5%TC*) produced slightly slower respiration rates compared to the other treated microcosms (total 415 and 393 mmol CO_2/kg, respectively). Higher doses of porous carbon (> 2%) may alter the ratios of carbon to inorganic nutrients (e.g., C: N: P ratio) and may make the treated soil coarser due to the sand particle size of the porous carbon, which results in lower soil respiration activity in general. However, 1% porous carbon in combination with zeolite and the nutrient solution (200N + 2%Z + 1%TC) enhanced soil respiration activity more than the zeolite and nutrient treatment without porous carbon (200N + 2%Z), especially for the initial boosting of microbial activity that can be observed in the soil CO_2 production rate profile (Figure 6). Soil CO_2 production in the treated soils decreased as the soils were frozen, but soil CO_2 production continued in all the treated soils and did not cease at sub-zero temperatures (0 to -10 °C).

Figure 5.

Figure 6.

3.3. Experimental SFCCs of treated contaminated soils

The soil biostimulation treatments modified the SFCCs of contaminated site soils. Figure 7 shows the experimental SFCC of the treated and untreated soils, along with those of reference soils from the literature, as similarly described in Kim et al., (2021). The general trend in the SFCCs reveals an upward shift in the curves of the site soils that received liquid nutrient and solid mineral amendments, reflecting greater unfrozen water retention during freezing due to elevated nutrient

solutes and increased surface area in the treated soils compared to the untreated soil (control), which was consistent with what was observed by Kim et al., (2021). In Figure 7, the SFCCs of treated soils are shifted upward toward the shaded region of the diagram corresponding to clayey soils compared to the SFCC of the untreated soils, which lie closest to the SFCC range of sandy soils. This correlates to the extension of unfrozen water availability in treated contaminated soils during freezing. The experimental SFCCs in Figure 7 were used for the SFCC-RESP model development.

Figure 7.

3.4. Simulated SFCCs of treated contaminated soils

Figure 8 shows the SFCCs simulated using the TEMP/W model, overlapped with the experimental SFCCs obtained from the soil freezing experiment. The simulated SFCCs were in good agreement with the experimental SFCCs (R^2= 0.98–0.99). The soil thermal model (TEMP/W) was thus calibrated for the treated soils and the observed SFCCs, which modified soil thermal phase change rates and unfrozen water retention. The calibrated soil thermal model produces modified SFCCs due to soil treatment and predicts unfrozen water retention under different soil treatment scenarios and seasonal freeze-thaw cycles. The calibrated model enables the prediction of unfrozen water retention in freezing and frozen hydrocarbon-contaminated soils by modifying the soil conditions that manipulate the thermal conductivity and heat capacity of treated soils amended with clay minerals (zeolite), nutrients and water (Supplementary Figures S3 and S4).

Figure 8.

3.5. Correlation between unfrozen water and respiration activity during soil freezing

Figure 9 shows overlapping profiles of soil temperature, unfrozen water content and CO_2 production measured over time in the *200N + 2%Z + 1%TC* microcosms. The temperature dependency of soil respiration activity is predominant in the unfrozen phase, above the freezing-depression point (FPD), as shown in Figure 9 (Pearson's correlation coefficient, r = 0.97), compared to the effect of unfrozen water content (r = 0.79). However, at temperatures below the FPD, in the freezing phase, unfrozen water availability became critical in regulating soil CO_2 gas production (r = 0.94) and comparable to the effect of temperature, which remained a driving factor of change in respiration activity (r = 0.90). The other treated soil microcosms exhibited similar correlations between CO_2 production and unfrozen water content at temperatures near and below their freezing points, as demonstrated by the analogous overlapping profiles of soil temperature, unfrozen water content and CO_2 production provided in Supplementary Figure S5, suggesting the coupling of temperature and unfrozen water effects on soil respiration activity during freezing.

Table 2 summarizes the result of the correlation analyses between CO_2 production and soil temperatures (T) and unfrozen water content (θ) as they were measured in all treated microcosms subjected to seasonal freezing. In the unfrozen phase (at soil temperatures above lowered freezing-point of the soils), measured CO_2 production rates in all treated soils decreased with soil temperature. As shown in the *Unfrozen phase* in Table 2, the correlation between CO_2 production and soil temperature is statistically significant, and the effect of soil temperature is predominant. Below the depressed freezing point of the soils (*Frozen Phase* in Table 2), the coefficients of the correlations between CO_2 production and unfrozen water content were significantly elevated in the treated microcosms samples, to 0.83–0.94 compared to 0.65–0.79 in the unfrozen phase, with

the exception of the *200N + 2%Z + 5%TC* microcosms, which exhibited slightly lower respiration activity due to the suboptimal treatment (i.e., high porous carbon dosage). Changes in unfrozen water availability in biostimulated, hydrocarbon-contaminated soils tended to regulate respiration activity upon the onset of soil freezing.

Table 2.

3.6. Temperature-dependent soil respiration models

Based on the CO_2 production data, the *200N+2%Z+1%TC* microcosms, which showed the highest CO_2 production rates (most microbial enhancement), were considered for further detailed analyses of the temperature dependency of respiration activity in biostimulated contaminated soil during simulated seasonal freezing. As shown in Figure 10(a), above 0 °C, the Arrhenius equation accounted for the exponential decrease in respiration activity as the soil temperature decreased. However, the deviation between the experimental data and the Arrhenius model extended to sub-zero temperatures became greater in the frozen phase (0 to -10 °C) when the soil phase change occurred. Figure 10(b) shows the Arrhenius equation produced a generally good fit to the CO_2 production data during the decrease in soil temperature from 4 to -10 °C, using non-linear curve-fitting at R^2 of 0.86 (RMSE: 0.003; MARE: 0.123). This reaffirms that temperature is the governing factor in regulating respiration activity during seasonal soil freezing. However, the modelled respiration curve did not accurately describe the abrupt drop in soil respiration activity near 0 °C upon the FPD at the onset of soil phase change or sub-zero respiration activity (Figure 10). Applying Q_{10}-based, temperature-dependent respiration models also suggested that temperature alone does not explain respiration responses in biologically

active contaminated soils at sub-zero temperatures (Supplementary Figure S6). The Arrhenius and Q_{10}-based respiration models were developed to account only for the temperature dependency of soil respiration and do not fully address the emerging influence of unfrozen water on soil respiration activity as the phase changes from unfrozen to frozen in cold climates.

Figure 10.

3.7. Incorporating the SFCC into respiration modelling for freezing soil (SFCC-RESP)

To address the observed correlation between unfrozen water content and respiration activity at sub-zero temperatures (Table 2), the equation for the soil-freezing characteristic curve (SFCC: $\theta = \alpha T^{\beta}$) was mathematically incorporated into the exponentially decreasing respiration function using a product of T and θ, the two interactive variables, as described in Eqs. (4) to (10). Table 3 presents separate respiration equations for soil temperatures above and below 0 °C used in the SFCC-RESP model. Above 0 °C, the strong temperature-dependency of respiration activity that was observed in this study and Kim and Chang, (2019) suggests that the Arrhenius equation can be applied without modification. Below 0 °C, however, the developed SFCC-RESP model can be applied to account for the coupled effects of soil temperature and unfrozen water content on respiration during freezing.

Table 3.

Figure 11 shows the results of applying the developed SFCC-RESP modelling to the freezing phase (0 to -10 °C) in biostimulated contaminated site soil (*200N+2%Z+1%TC*

microcosm), in conjunction with the Arrhenius equation for the unfrozen phase (4 to 0 °C). The combined respiration models produced a good fit with an R^2 of 0.97, RMSE of 0.001, and MARE of 0.038, an improved output compared to the respiration models that only consider the temperature-dependency of soil respiration. The SFCC-RESP model described the abrupt drop in soil respiration at T_o = -2.6 °C, which correlated with the sudden drop in unfrozen water content at the FPD of -1 °C in the biostimulated soil. The SFCC-RESP model successfully addresses the limitation of the Arrhenius equation to delineate changes in sub-zero CO_2 respiration activity influenced by soil temperature and unfrozen water content in freezing biostimulated contaminated soils (*200N+2%Z+1%TC* microcosm).

Figure 11.

3.8. Sensitivity analysis of the SFCC-RESP model for soil thermal phase change

The *k* term in the SFCC-RESP is a curve-fitting constant relating the response in respiration activity to decreasing unfrozen water availability during soil freezing. Figure 12 presents the sensitivity analysis outputs for the SFCC-RESP model produced by manipulating *k* values to produce the best fit to the experimental CO_2 data measured in the biostimulated, contaminated soil microcosms (*200N+2%Z+1%TC*) during soil thermal phase change (0 to -7 °C). The *k* is an exponent of the exponential function in the SFCC-RESP equations in Table 3 and control the abruptness of the decrease in CO_2 production at given T_o and α values specific to the soil. The *k* term is expressed as the inverse of the product of temperature (°C) and unfrozen water content (m^3/m^3), $\frac{1}{[T][L^3/L^3]}$. The *k* value in the SFCC-RESP model essentially controls the curvature of the decreasing respiration curve at sub-zero temperatures. Higher *k* values describe sharper decreases

in respiration activity, whereas lower *k* values produce more gradual reductions in respiration under the same conditions. As shown in Figure 12(a), manipulated *k* values between 9 and 90 were entered into the SFCC-RESP model. Other parameters determined for the *200N+2%Z+1%TC* microcosm (e.g., T_0, α and β) were held constant for the SFCC-RESP model sensitivity analyses, as shown in Supplementary Table S3. The sensitivity analysis revealed that higher *k* values describe more abrupt decreases in respiration activity associated with the earlier onset of limited unfrozen water and soil temperatures reaching colder negative temperatures. In contrast, lower *k* values were associated with prolonged respiration activity and the extended availability of unfrozen water during freezing. As shown in Figure 12(b), the sensitivity analysis selected a *k* value of 57.09 based on the highest R^2 of 0.83, the best fit to the experimental CO_2 production data for the *200N + 2%Z + 1%TC* microcosms measured during the soil phase change from unfrozen to frozen.

Figure 12.

The SFCC-RESP model can also be used to demonstrate the extension of respiration activity to colder temperatures in freezing soils as the model is assigned lower T_o values (the critical soil temperature at which CO_2 production abruptly drops) and higher α values (a constant parameter of the SFCC equation that is related to soil type). Figure 13(a) is an example simulation with manipulated T_o and α values, which are both associated with unfrozen water retention during freezing. Lowering T_o values from -2.6 to -5 and -7 °C produces increasing α values from 0.05 to 0.08 and 0.1, respectively, using the *k* value of 57.09 selected for the *200N+2%Z+1%TC* microcosms. The α value (unitless) reflects characteristics related to soil

type and unfrozen water retention (Kim et al., 2021) and thus the SFCC equation (i.e., $\theta = \alpha T^{\beta}$) is incorporated into the SFCC-RESP equation. Generally, soils with higher α values retain more unfrozen water content during freezing (Kim et al., 2021). The SFCC-RESP model inversely formulates that if soils can be treated to possess a higher α value, those treated soils will retain more unfrozen water during freezing and exhibit a lower T_0 value at a given *k*, therefore extending the simulated respiration activity at sub-zero temperatures. The β parameter in the common SFCC equation also controls the extension of respiration activity in the SFCC-RESP model, similarly to α; however, the model is less sensitive to β values than it is to α values (Figure 13(b)). In the SFCC equation, β is a fitting constant that is an experimental parameter, as was determined experimentally for various soil types, from clays to sands (Andersland & Ladanyi 2003).

Figure 13.

3.9. Simulated spatial distributions of T, θ, and CO_2 (SFCC-RESP and TEMP/W)

The SFCC-RESP model is expressed as a function of T and θ (or α and β) to calculate respiration rate. Using the experimental SFCC for the *200N+2%Z+1%TC* microcosms (Figure 7), the TEMP/W model simulated T and θ responses over time as the microcosms were subjected to freezing stress. The simulated T and θ showed a good fit with the corresponding experimental T and θ (Figure 8). Using the simulated SFCC data, the numerical soil thermal model (TEMP/W) produced high-throughput transient datasets for T and θ for each element in the mesh domain of the *200N+2%Z+1%TC* microcosm (i.e., 551 data points for T and θ at each time step, for 132-time steps, generating a total of 72,732 data points over the 11-day period of freezing below the

freezing-point depressions; Supplementary Figure S7). The validated high-throughput datasets for T and θ allowed us to produce spatial distributions of T and θ in the microcosms during freezing. Figures 14(a) and 14(b) show snapshots of the simulated spatial distributions of T and θ when sub-zero respiration activity in the *200N+2%Z+1%TC* microcosms decreased abruptly between -3 and -5 °C (partially frozen and frozen phases). These T and θ datasets for the *200N+2%Z+1%TC* microcosms were then fed into the SFCC-RESP equation, and corresponding CO_2 production rates were computed, producing simulated spatial distributions of CO_2 production rates in the microcosms during freezing (Figure 14(c)). Overall, the modelling approach combining SFCC-RESP and TEMP/W was validated specifically for the *200N+2%Z+1%TC* microcosms and produced 2D information on soil temperature, unfrozen water content, and CO_2 production rates in the treated microcosms subjected to seasonal freezing stress.

Figure 14.

3.10. Applications of SFCC-RESP to other soil treatments

The modelling approach combining the SFCC-RESP and TEMP/W models was also applied to the other microcosms run in this study, as the outputs of the combined modelling were validated using the experimental and simulated datasets for the *200N+2%Z+1%TC* microcosms (Section 3.9). The experimental SFCCs for each microcosm treated with nutrient and mineral amendments were produced and used as the input parameters for the SFCC-RESP and TEMP/W modelling (Figure 7 for 2*00N+2%Z*, *200N+2%Z+2%TC* and *200N+2%Z+5%TC* microcosms). As shown in Figure 15, the Arrhenius equation was applied above 0 °C, and the SFCC-RESP model was applied below 0 °C, which produced an excellent fit with the experimental CO_2

production rates measured in the treated microcosms (R^2 values of 0.94 to 0.98 for the combined Arrhenius–SFCC-RESP model). The input parameters for the SFCC-RESP model are presented in detail in Supplementary Table S4.

Figure 15.

Following this validation of the SFCC-RESP model for each microcosm, the TEMP/W model was applied to generate the high-throughput, simulated datasets for T and θ for each of the treated microcosms (Supplementary Figures S7 and S8), which were then fed into the SFCC-RESP model to simulate CO_2 production rates in each microcosm (Supplementary Figure S9). The spatial distributions of T and θ values and corresponding CO_2 production rates in the microcosms were then produced using the generated datasets. Figure 16 shows a snapshot of computed CO_2 production rates for the three microcosm sets that received soil treatments and exhibited significant CO_2 production at approximately -3 °C in the partially frozen phase when unfrozen water and pore ice coexisted (3 days after soil temperatures dropped below the depressed freezing-point of the soil water). The simulated spatial distributions of CO_2 production rates in the different treated soil microcosms suggested that the *200N + 2%Z + 1%TC* treatment yielded the highest respiration activity compared to the others (*200N + 2%Z* and *200N + 2%Z + 2%TC*), which is in a good agreement with the experimental respiration data shown in Figures 5 and 6.

Figure 16.

4. Discussion

Soil temperature was a governing factor in regulating soil respiration activity (soil CO_2 production rate) under the simulated seasonal freezing conditions (4 to -10 °C at -1 °C/day), which was represented by the exponential function in the SFCC-RESP equation. However, the role of unfrozen water becomes critical upon seasonal soil freezing, and unfrozen water content is statistically significantly correlated with the abrupt decrease in soil respiration activity (Table 2). Changes in unfrozen water content during the seasonal soil phase change can be used to predict the effective inflection point, or abrupt decrease, in the onset of sub-zero soil CO_2 respiration activity. In this study, this relationship between unfrozen water and soil respiration was empirically approximated by incorporating the SFCC equation, which is specific to the treated site soils, into the exponential expression of the temperature-governed soil respiration model. This SFCC-based approach successfully coupled the effects of freezing temperatures and unfrozen water on CO_2 production in hydrocarbon-contaminated soils treated for cold-tolerant biostimulation, which produced the framework for the new SFCC-RESP model.

This SFCC-based approach is comparable to the URESP model developed by Kim and Chang, (2019), which similarly describes the coupled effects of temperature and unfrozen water on soil respiration activity in biostimulated, petroleum-contaminated sandy soils under seasonal thawing conditions. The URESP model for sub-zero respiration activity was based on the Michaelis-Menten equation, a substrate-based microbial kinetic model, and on the underlying assumption that substrate availability (hydrocarbons) decreases proportionally as unfrozen water content decreases under soil freeze-thaw conditions. This assumption was valid when the substrates were in the aqueous phase, and the URESP model was in good agreement with the experimental data obtained for the sandy soils (Kim & Chang 2019). In this URESP model, a decrease in liquid unfrozen water content due to soil freezing is assumed to correspond with a

decrease in the dissolved substrates available for microbial uptake. This critical concept in the development of the URESP model led to the *intuitive* new approach proposed in this study for improving sub-zero respiration modelling, which considers the fundamental expression of the freezing soil characteristics and associated unfrozen water retention in the form of the soil-freezing characteristic curve. This present study suggests that the SFCCs of contaminated soils treated for bioremediation can be incorporated into the Arrhenius-based, temperature-dependent soil respiration models to directly address time-variable freezing soil temperature and unfrozen water effects on sub-zero respiration activity during seasonal freezing. The SFCC is expressed as a function of soil temperature and unfrozen water (or matric potential), the two critical variables in conventional soil respiration models. The SFCC of soils treated for bioremediation reflects how the soil freezing characteristics, including unfrozen water retention and prolonged partially frozen phase, are altered due to the soil treatment. Additionally, SFCC information for diverse soil types is available in the literature and may also be used as input data to the SFCC-RESP models. This study suggests that the SFCC is a direct and simple tool that can be used in soil respiration modelling to predict changes in sub-zero soil CO_2 respiration activity in cold-region hydrocarbon-contaminated soils treated for bioremediation.

The upward shifting in the SFCCs of the treated contaminated soils in this study reflects that the soil treatments extend unfrozen water availability and may increase the abundance of unfrozen habitable niches for microbial activity due to increased solute concentrations of supplied nutrients and added surface area from zeolite minerals. The shifts in SFCCs of the treated hydrocarbon-contaminated soils towards the SFCCs of clayey soils are associated with greater unfrozen water retention under the simulated seasonal freezing conditions, making the soils more favourable to hydrocarbon biodegradation extended to colder temperatures (Kim et al.

2021). Clayey soils provide more microsites for unfrozen water retention resulting in the lower effective endpoint of partially frozen phase and extending sub-zero microbial activity compared to sandy soils (Kim et al. 2021). Bioremediation strategies extended for sub-zero temperature regime (e.g., seasonal freezing condition) can be optimized for enhanced winter microbial activity. As the α value in the SFCC equation ($\theta = \alpha T^{\beta}$) approached 0.1 in the treated soils in Kim et al. (2021), closer to the α values of clays, hydrocarbon biodegradation under seasonal freezing conditions was greater. Therefore, predicting and visualizing the spatial distribution of unfrozen water in treated soils is meaningful in developing the cold-tolerant bioremediation strategies extended beyond conventional treatment seasons. In the present study, the different soil treatments tested modified the SFCC of the original untreated soil, and changed unfrozen water retention, suggesting the possibility of comparing and adjusting soil amendments with the objective of extending hydrocarbon biodegradation in contaminated soils at sub-zero temperatures.

The SFCC-RESP model indicates the inflection point in soil respiration activity during the soil phase transition. This inflection point may be regarded as a critical point in the seasonal turnover from summer to winter microbial communities in soils, rather than as the seasonal inactivation of microbial activity. Both laboratory and field studies observed seasonal shifts in microbial community in both treated and untreated hydrocarbon-contaminated soils (Chang et al. 2011a, Kim et al. 2018). While bulk measurable soil respiration activity is notably depressed in the early freezing phase, when unfrozen water is still significantly detectable, hydrocarbon biodegradation does not cease as treated soils freeze further, as shown in previous studies (Chang et al. 2011a, Kim et al. 2018). Freezing-tolerant hydrocarbon-degrading bacteria emerge with the seasonal phase change from unfrozen to partially frozen in contaminated soils treated with

nutrients and/or minerals (Chang et al. 2011a, Kim et al. 2018). Rike et al., (2005, 2003) suggest a diffusion-based model stating that seasonal profiles of soil CO_2 and O_2 gas concentrations can be related to the seasonal inactivation and activation of bulk microbial activity in hydrocarbon-contaminated soils, but does not consider the influence of unfrozen water on respiration activity below 0 °C.

The SFCC-RESP model introduces the *k* term, expressed as an inverse to the product of temperature (*T*) and unfrozen water term (θ), to simulate the inflection point in soil respiration activity during the soil thermal phase change at seasonal soil freezing rates. The sensitivity analysis of *k* values for the site soils shows that this parameter reflects the abruptness of the decreasing in soil respiration activity and may be useful in formulating soil treatments that will enhance respiration activity in the field specifically during the seasonal phase change from unfrozen to deeply frozen. The SFCC-RESP model may therefore be applicable for adjusting soil treatments for optimized SFCC parameters (α and β) and maximizing respiration activity in treated hydrocarbon-contaminated soils in cold climates. The SFCC-RESP model integrated with TEMP/W may provide a tool to predict unfrozen water retention through the optimized SFCCs of various soils treated for bioremediation, to estimate the coupled effects of temperature and unfrozen water retention on respiration activity during soil freezing, and to assist in the development of cold-tolerant bioremediation strategies, as proposed in Kim et al. (2021).

5. Conclusion

In this study, an induced-freezing soil microcosm experiment indicated that the soil treatment used for biostimulation (nutrients, zeolite and porous carbon) enhanced soil respiration activity (CO_2 production rate) under simulated seasonal freezing conditions (4 to -10 °C at -1 °/day). The

zeolite amendment in the soil treatment for bioremediation is beneficial to microbial survival in contaminated soils under water scarcity. The biostimulation treatment also modified the SFCC of the contaminated soils, reflecting the enhanced retention of unfrozen water during freezing. By incorporating the SFCC into soil respiration modelling, this study produced the SFCC-RESP model that closely approximated the measured soil CO_2 respiration in seasonally freezing biostimulated, petroleum hydrocarbon-contaminated soils by accounting for the effects of both temperature and unfrozen water below 0 °C. The SFCC-RESP model predicted the seasonal inflection point in soil respiration activity with improved accuracy. Using both the SFCC-RESP model and numerical soil thermal modelling (TEMP/W) calibrated for the treated soils in this study, spatial distributions of unfrozen water, soil temperature and corresponding CO_2 production rates were generated for the microcosms. This study suggests that calibrated SFCC-RESP and TEMP/W models have the potential to be useful in developing cold-climate bioremediation strategies for hydrocarbon-contaminated soils at remote sites and for assessing the seasonality of soil respiration activity in freezing and frozen soils. The SFCC-RESP model is an empirical model framework developed based on experimental data for soil respiration under induced freezing at the microcosm scale. The SFCC-RESP model can be developed and improved further in future studies by exploring modifications in the SFCC associated with other contaminated soils, soil treatments, and various seasonal freeze-thaw conditions.

Supplementary Information

The online version contains supplementary information available at htttps://

Acknowledgement

We extend special thanks to LuVerne E. W. Hogg (ZMM® Canada Minerals Corp.) for providing the zeolite and porous carbon amendments for soil treatment and the corresponding material properties data.

Author contribution Methodology, development, and investigation, data acquisition, and data analysis: Tasnim Nayeema, Methodology, investigation, and data acquisition: Aslan Hwanhwi Lee, Writing—original draft preparation: Tasnim Nayeema, Writing— reviewing and editing: Wonjae Chang, Amy Richter, Kelvin Tsun Wai Ng, Conceptualization, design and funding acquisition: Wonjae Chang.

Funding This study was supported by ZMM® Canada Minerals Corp. and Mitacs Accelerate Grant (IT12123 granted to Wonjae Chang).

Data availability The authors declare that all relevant data that support the findings of this study are available within the article, including the supplementary information. Additional data are available from the corresponding author upon reasonable request.

Declarations

Ethics approval Not applicable.

Consent to participate All authors have consented to participation.

Consent for publication All authors have consented to publication.

Competing interests The authors have no competing interests to declare that are relevant to the content of this article.

References

Aislabie J, Saul DJ, Foght JM (2006) Bioremediation of hydrocarbon-contaminated polar soils. Extremophiles 10, 171-179, https://doi.org/10.1007/s00792-005-0498-4

Aislabie JM, Balks MR, Foght JM, Waterhouse EJ (2004) Hydrocarbon Spills on Antarctic Soils: Effects and Management. Environ Sci Tech 38, 1265-1274, https://doi.org/10.1021/es0305149

Andersland OB, Ladanyi B (2003): Frozen Ground Engineering. American Society of Civil Engineers (ASCE), John Wiley & Sons, Hoboken, New Jersey

Anderson DM, Tice AR, McKim HL (1973): The unfrozenwater and the apparent specific heat capacity of frozen soils, Second International Conference on Permafrost. North American Contribution. National Academy of Sciences, Yakutsk, USSR

Aspray T, Gluszek A, Carvalho D (2008) Effect of nitrogen amendment on respiration and respiratory quotient (RQ) in three hydrocarbon contaminated soils of different type. Chemosphere 72, 947-951, https://doi.org/10.1016/j.chemosphere.2008.03.017

Børresen MH, Barnes DL, Rike AG (2007) Repeated freeze–thaw cycles and their effects on mineralization of hexadecane and phenanthrene in cold climate soils. Cold Reg Sci Technol 49, 215-225, https://doi.org/10.1016/j.coldregions.2007.02.001

Braddock JF, Ruth ML, Catterall PH, Walworth JL, McCarthy KA (1997) Enhancement and inhibition of microbial activity in hydrocarbon-contaminated Arctic soils: Implications for nutrient-amended bioremediation. Environ Sci Tech 31, 2078-2084, https://doi.org/10.1021/es960904d

Byun E, Rezanezhad F, Fairbairn L, Slowinski S, Basiliko N, Price JS, Quinton WL, Roy-Léveillée P, Webster K, Van Cappellen P (2021) Temperature, moisture and freeze–thaw controls on CO_2 production in soil incubations from northern peatlands. Sci Rep 11, 23219, https://doi.org/10.1038/s41598-021-02606-3

Chang W, Dyen M, Spagnuolo L, Simon P, Whyte L, Ghoshal S (2010) Biodegradation of semi- and non-volatile petroleum hydrocarbons in aged, contaminated soils from a sub-Arctic site: Laboratory pilot-scale experiments at site temperatures. Chemosphere 80, 319-326, https://doi.org/10.1016/j.chemosphere.2010.03.055

Chang W, Klemm S, Beaulieu C, Hawari J, Whyte L, Ghoshal S (2011a) Petroleum hydrocarbon biodegradation under seasonal freeze−thaw soil temperature regimes in contaminated soils from a sub-Arctic Site. Environ Sci Technol 45, 1061-1066, https://doi.org/10.1021/es1022653

Chang W, Whyte L, Ghoshal S (2011b) Comparison of the effects of variable site temperatures and constant incubation temperatures on the biodegradation of petroleum hydrocarbons in pilot-scale experiments with field-aged contaminated soils from a cold regions site. Chemosphere 82, 872-8, https://doi.org/10.1016/j.chemosphere.2010.10.072

Chang W, Ghoshal S (2014) Respiratory quotients as a useful indicator of the enhancement of petroleum hydrocarbon biodegradation in field-aged contaminated soils in cold climates. Cold Reg Sci Technol 106, 110-119, https://doi.org/10.1016/j.coldregions.2014.06.010

Chang W, Akbari A, David C, Ghoshal S (2018) Selective biostimulation of cold- and salt-tolerant hydrocarbon-degrading *Dietzia maris* in petroleum-contaminated sub-Arctic soils

with high salinity. J Chem Technol Biotechnol 93, 294-304, https://doi.org/10.1002/jctb.5385

Coulon F, Pelletier E, St Louis R, Gourhant L, Delille D (2004) Degradation of petroleum hydrocarbons in two sub-antarctic soils: Influence of an oleophilic fertilizer. Environ Toxicol Chem 23, 1893-901, https://doi.org/10.1897/03-484

Davidson EA, Janssens IA, Luo Y (2006) On the variability of respiration in terrestrial ecosystems: moving beyond Q10. Glob Chang Biol 12, 154-164, https://doi.org/10.1111/j.1365-2486.2005.01065.x

Deming JW (2002) Psychrophiles and polar regions. Curr Opin Microbiol 5, 301-309, https://doi.org/10.1016/S1369-5274(02)00329-6

Devoie ÉG, Gruber S, McKenzie JM (2022) A repository of measured soil freezing characteristic curves: 1921 to 2021. Earth Syst Sci Data 14, 3365-3377, https://doi.org/10.5194/essd-14-3365-2022

Drotz HS, Tilston EL, Sparrman T, Schleucher J, Nilsson M, Öquist MG (2009) Contributions of matric and osmotic potentials to the unfrozen water content of frozen soils. Geoderma 148, 392-398, https://doi.org/10.1016/j.geoderma.2008.11.007

Elberling B, Brandt KK (2003) Uncoupling of microbial CO_2 production and release in frozen soil and its implications for field studies of arctic C cycling. Soil Biol Biochem 35, 263-272, https://doi.org/10.1016/S0038-0717(02)00258-4

Eriksson M, Ka JO, Mohn WW (2001) Effects of low temperature and freeze-thaw cycles on hydrocarbon biodegradation in Arctic tundra soil. Appl Environ Microbiol 67, 5107-12, https://doi.org/10.1128/AEM.67.11.5107-5112.2001

Farouki OT (1981) The thermal properties of soils in cold regions. Cold Reg Sci Technol 5, 67-75, https://doi.org/10.1016/0165-232X(81)90041-0

FCSI (2023) Federal Contaminated Sites Inventory. https://www.tbs-sct.gc.ca/fcsi-rscf/home-accueil-eng.aspx 2023

Gomez F, Sartaj M (2013) Field scale ex-situ bioremediation of petroleum contaminated soil under cold climate conditions. Int Biodeter Bioder 85, 375-382, https://doi.org/10.1016/j.ibiod.2013.08.003

Harris NJ (2017) Hypersaline potash mine tailings and brine: microbial communities and metal biosorption applications. Thesis, University of Saskatchewan

Harris NJ, Dynes JJ, McBeth JM, Patel M, Chang W (2023) Waste biomass from hypersaline potash mining byproducts: Detection and visualization of Cu(II) and Cr(VI) on *Croceicoccus* sp. FTI14 biosorbent. Waste Manag Bull 1, 45-57, https://doi.org/10.1016/j.wmb.2023.07.001

Karppinen EM, Siciliano SD, Stewart KJ (2017a) Application method and biochar type affect petroleum hydrocarbon degradation in northern landfarms. J Environ Qual 46, 751-759, https://doi.org/10.2134/jeq2017.01.0038

Karppinen EM, Stewart KJ, Farrell RE, Siciliano SD (2017b) Petroleum hydrocarbon remediation in frozen soil using a meat and bonemeal biochar plus fertilizer. Chemosphere 173, 330-339, https://doi.org/10.1016/j.chemosphere.2017.01.016

Karppinen EM, Mamet SD, Stewart KJ, Siciliano SD (2019) The charosphere promotes mineralization of ^{13}C-phenanthrene by psychrotrophic microorganisms in Greenland soils. J Environ Qual 48, 559-567, https://doi.org/10.2134/jeq2018.10.0370

Kim J, Lee AH, Chang W (2018) Enhanced bioremediation of nutrient-amended, petroleum hydrocarbon-contaminated soils over a cold-climate winter: The rate and extent of hydrocarbon biodegradation and microbial response in a pilot-scale biopile subjected to natural seasonal freeze-thaw temperatures. Sci Total Environ 612, 903-913, https://doi.org/10.1016/j.scitotenv.2017.08.227

Kim J, Chang W (2019) Modified soil respiration model (URESP) extended to sub-zero temperatures for biostimulated petroleum hydrocarbon-contaminated sub-Arctic soils. Sci Total Environ 667, 400-411, https://doi.org/10.1016/j.scitotenv.2019.02.067

Kim J, Lee AH, Chang W (2021) Manipulation of unfrozen water retention for enhancing petroleum hydrocarbon biodegradation in seasonally freezing and frozen soil. Environ Sci Tech 55, 9172-9180, https://doi.org/10.1021/acs.est.0c07502

Konrad J-M, McCammon A (1990) Solute partitioning in freezing soils. Can Geotech J 27, 726-736, https://doi.org/10.1139/t90-086

Lellei-Kovács E, Botta-Dukát Z, de Dato G, Estiarte M, Guidolotti G, Kopittke GR, Kovács-Láng E, Kröel-Dulay G, Larsen KS, Peñuelas J, Smith AR, Sowerby A, Tietema A, Schmidt IK (2016) Temperature Dependence of Soil Respiration Modulated by Thresholds in Soil Water Availability Across European Shrubland Ecosystems. Ecosyst 19, 1460-1477, https://doi.org/10.1007/s10021-016-0016-9

Lloyd J, Taylor J (1994) On the temperature dependence of soil respiration. Funct Ecol https://doi.org/10.2307/2389824, 315-323, https://doi.org/10.2307/2389824

Ma T, Wei C, Xia X, Zhou J, Chen P (2017) Soil freezing and soil water retention characteristics: connection and solute effects. J. Perform Constr Facil 31, D4015001, https://doi.org/10.1061/(ASCE)CF.1943-5509.0000851

Mair J, Schinner F, Margesin R (2013) A feasibility study on the bioremediation of hydrocarbon-contaminated soil from an Alpine former military site: Effects of temperature and biostimulation. Cold Reg Sci Technol 96, 122-128, https://doi.org/10.1016/j.coldregions.2013.07.006

Makita N, Kosugi Y, Sakabe A, Kanazawa A, Ohkubo S, Tani M (2018) Seasonal and diurnal patterns of soil respiration in an evergreen coniferous forest: Evidence from six years of observation with automatic chambers. PLOS ONE 13, e0192622, https://doi.org/10.1371/journal.pone.0192622

Margesin R (2000) Potential of cold-adapted microorganisms for bioremediation of oil-polluted Alpine soils. Int Biodeter Bioder 46, 3-10, https://doi.org/10.1016/S0964-8305(00)00049-4

Margesin R, Schinner F (2001) Biodegradation and bioremediation of hydrocarbons in extreme environments. Appl Microbiol Biotechnol 56, 650-663, https://doi.org/10.1007/s002530100701

Martínez Álvarez LM, Ruberto LAM, Lo Balbo A, Mac Cormack WP (2017) Bioremediation of hydrocarbon-contaminated soils in cold regions: Development of a pre-optimized biostimulation biopile-scale field assay in Antarctica. Sci Total Environ 590-591, 194-203, https://doi.org/10.1016/j.scitotenv.2017.02.204

Martínez Álvarez LM, Ruberto LAM, Gurevich JM, Mac Cormack WP (2020) Environmental factors affecting reproducibility of bioremediation field assays in Antarctica. Cold Reg Sci Technol 169, 102915, https://doi.org/10.1016/j.coldregions.2019.102915

Martínez Álvarez LM, Bolhuis H, Mau GK, Kok-Gan C, Sing CC, Mac Cormack W, Ruberto L (2022) Identification of key bacterial players during successful full-scale soil field bioremediation in Antarctica. Int Biodeter Bioder 168, 105354, https://doi.org/10.1016/j.ibiod.2021.105354

McCarthy K, Walker L, Vigoren L, Bartel J (2004) Remediation of spilled petroleum hydrocarbons by in situ landfarming at an arctic site. Cold Reg Sci Technol 40, 31-39, https://doi.org/10.1016/j.coldregions.2004.05.001

Miri S, Naghdi M, Rouissi T, Kaur Brar S, Martel R (2019) Recent biotechnological advances in petroleum hydrocarbons degradation under cold climate conditions: A review. Crit Rev Environ Sci Technol 49, 553-586, https://doi.org/10.1080/10643389.2018.1552070

Moinet GY, Hunt JE, Kirschbaum MU, Morcom CP, Midwood AJ, Millard P (2018) The temperature sensitivity of soil organic matter decomposition is constrained by microbial access to substrates. Soil Biol Biochem 116, 333-339, https://doi.org/10.1016/j.soilbio.2017.10.031

Mundim KC, Baraldi S, Machado HG, Vieira FMC (2020) Temperature coefficient (Q10) and its applications in biological systems: Beyond the Arrhenius theory. Ecol Modell 431, 109127, https://doi.org/10.1016/j.ecolmodel.2020.109127

Nikrad MP, Kerkhof LJ, Häggblom MM (2016) The subzero microbiome: microbial activity in frozen and thawing soils. FEMS Microbiol Ecol 92, fiw081, https://doi.org/10.1093/femsec/fiw081

Öquist MG, Sparrman T, Klemedtsson L, Drotz SH, Grip H, Schleucher J, Nilsson M (2009) Water availability controls microbial temperature responses in frozen soil CO_2 production. Glob Change Biol 15, 2715-2722, https://doi.org/10.1111/j.1365-2486.2009.01898.x

Panikov N, Flanagan P, Oechel W, Mastepanov M, Christensen T (2006) Microbial activity in soils frozen to below -39 °C. Soil Biol Biochem 38, 785-794, https://doi.org/10.1016/j.soilbio.2005.07.004

Paudyn K, Rutter A, Rowe RK, Poland JS (2008) Remediation of hydrocarbon contaminated soils in the Canadian Arctic by landfarming. Cold Reg Sci Technol 53, 102-114, https://doi.org/10.1016/j.coldregions.2007.07.006

Qi Y, Xu M, Wu J (2002) Temperature sensitivity of soil respiration and its effects on ecosystem carbon budget: nonlinearity begets surprises. Ecol Modell 153, 131-142, https://doi.org/10.1016/S0304-3800(01)00506-3

Rike AG, Haugen KB, Børresen M, Engene B, Kolstad P (2003) *In situ* biodegradation of petroleum hydrocarbons in frozen arctic soils. Cold Reg Sci Technol 37, 97-120, https://doi.org/10.1016/S0165-232X(03)00005-3

Rike AG, Haugen KB, Engene B (2005) *In situ* biodegradation of hydrocarbons in arctic soil at sub-zero temperatures—field monitoring and theoretical simulation of the microbial activation temperature at a Spitsbergen contaminated site. Cold Reg Sci Technol 41, 189-209, https://doi.org/10.1016/j.coldregions.2004.10.005

Rivkina E, Friedmann E, McKay C, Gilichinsky D (2000) Metabolic activity of permafrost bacteria below the freezing point. Appl Environ Microbiol 66, 3230-3233, https://doi.org/10.1128/AEM.66.8.3230-3233.2000

Siciliano SD, Schafer AN, Forgeron MAM, Snape I (2008) Hydrocarbon contamination increases the liquid water content of frozen Antarctic soils. Environ Sci Tech 42, 8324-8329, https://doi.org/10.1021/es801731z

Snape I, Acomb L, Barnes DL, Bainbridge S, Eno R, Filler DM, Plato N, Poland JS, Raymond TC, Rayner JL, Riddle MJ, Rike AG, Rutter A, Schafer AN, Siciliano SD, Walworth JL (2008): Contamination, regulation, and remediation: an introduction to bioremediation of petroleum hydrocarbons in cold regions. In: Filler DM, Snape I , Barnes DL (Editors), Bioremediation of Petroleum Hydrocarbons in Cold Regions. Cambridge University Press, Cambridge, pp. 1-37

Tilston E, Sparrman T, Öquist M (2010) Unfrozen water content moderates temperature dependence of sub-zero microbial respiration. Soil Biol Biochem 42, 1396-1407, https://doi.org/10.1016/j.soilbio.2010.04.018

Walworth J, Braddock J, Woolard C (2001) Nutrient and temperature interactions in bioremediation of cryic soils. Cold Reg Sci Technol 32, 85-91, https://doi.org/10.1016/S0165-232X(00)00020-3

Wen Z, Ma W, Feng W, Deng Y, Wang D, Fan Z, Zhou C (2012) Experimental study on unfrozen water content and soil matric potential of Qinghai-Tibetan silty clay. Environ Earth Sci 66, 1467-1476, https://doi.org/10.1007/s12665-011-1386-0

Whyte LG, Goalen B, Hawari J, Labbé D, Greer CW, Nahir M (2001) Bioremediation treatability assessment of hydrocarbon-contaminated soils from Eureka, Nunavut. Cold Reg Sci Technol 32, 121-132, https://doi.org/10.1016/S0165-232X(00)00025-2

Yoshikawa K, Overduin PP (2005) Comparing unfrozen water content measurements of frozen soil using recently developed commercial sensors. Cold Reg Sci Technol 42, 250-256, https://doi.org/10.1016/j.coldregions.2005.03.001

Figure Caption

Figure 1. Freezing soil microcosms in a low-temperature programmable incubator equipped with temperature sensors, water content sensors, and soil gas ports, used in the freezing-induced soil respiration experiments

Figure 2. Overall workflow for developing the SFCC-RESP model.

Figure 3. Integrated CO_2 production rate and SFCC ($\theta = \alpha T^{\beta}$) for the determination of T_o, θ_o, r_i, and r_p in the SFCC-RESP model.

Figure 4. Diesel-spiked sands amended with zeolites and nutrient solutions and inoculated with *Dietzia maris* were subjected to drying stress: (a) the volumetric water content in the sand sets during soil drying and in the control set not subjected to drying, (b) the effect of zeolite (0% or 5% w/w) on microbial survival, enumerated after drying, at varying initial water contents (12.5%, 15%, 17.5% and 20% v/v); and (c) effect of zeolite dosage (0, 1, 2, 5 and 10% w/w) on microbial survival at 15% initial water content. ** indicates data that are statistically significantly different from the numbers of survivors (> 10^6 CFU/g) in the control set without the water scarcity stress.

Figure 5. Total soil CO_2 produced in the treated and untreated microcosms subjected to seasonal freezing from 4 to −10 °C at a rate of −1 °C/day

Figure 6. Temporal changes in soil CO_2 respiration rates in the treated and untreated microcosms subjected to seasonal freezing from 4 to -10 °C at -1 °C/day.

Figure 7. Experimental SFCCs of the treated and untreated contaminated soils, compared with those of several reference soils from the literature.

Figure 8. Simulated SFCCs of the treated contaminated soils, compared with those of soil-freezing experiments

Figure 9. Overlapping profiles of soil temperature, unfrozen water content and average CO_2 production rate measured in the biostimulated *200N + 2%Z + 1%TC* microcosms during the soil freezing experiment (4 to -10 °C at -1 °C/day). As indicated by the dotted lines, the soil phase transition was divided into the unfrozen and freezing/frozen phases for separate correlation analyses using Pearson's correlation coefficient, *r*.

Figure 10. Measured CO_2 production rates during induced seasonal freezing in biostimulated contaminated soils (*200N + 2%Z + 1%TC*) and those calculated using Arrhenius equation (temperature-dependent model) fitted to (a) the unfrozen soil phase only (4 to 0 °C) and (b) the entire range of soil temperatures (4 to -10 °C) reflecting the emergence of the role of unfrozen water in sustaining microbial respiration upon freezing.

Figure 11. Arrhenius and SFCC-RESP modelling of CO_2 production in the biostimulated hydrocarbon-contaminated soil (*200N + 2%Z + 1%TC*) above and below 0 °C, respectively, during induced seasonal freezing.

Figure 12. Sensitivity analysis of the SFCC-RESP model for fitting constant, *k*, showing (a) the model outputs for various input *k* values controlling the abruptness of the decrease in CO_2 production in biostimulated, contaminated soil during soil thermal phase change from unfrozen to partially frozen phase (0 to -7 C), and (b) the R^2 values associated with those *k* values.

Figure 13. Sensitivity analysis for α and β values. (a) manipulation of T_o and α values at a given *k* value in simulating CO_2 production rates during soil thermal phase change. (b) manipulation of β values at given *k* and α values in the simulation of CO_2 production rates extended to sub-zero temperatures.

Figure 14. The spatial distributions of (a) soil temperature, *T*, and (b) unfrozen water content, θ, and (c) the corresponding CO_2 production rates computed using the SFCC-RESP model fed with the *T* and θ *datasets* simulated using TEMP/W. The datasets represent soil temperatures between -2.9 and -5 °C (frozen phase below FDP), which occurred on Day 8 after the start of the induced-freezing experiment in the *200N + 2%Z + 1%TC* microcosms subjected to seasonal freezing.

Figure 15. Application of the Arrhenius equation in the unfrozen phase and the SFCC-RESP model in the frozen phase to simulate CO_2 production rates during seasonal freezing in the site soils that received the different nutrient and mineral amendments.

Figure 16. The spatial distributions of CO_2 production rates 3 days after soil temperatures dropped below the depressed freezing-point of the soil water in the different treated soil microcosms generated using high-throughput SFCC-RESP and TEMP/W modelling.

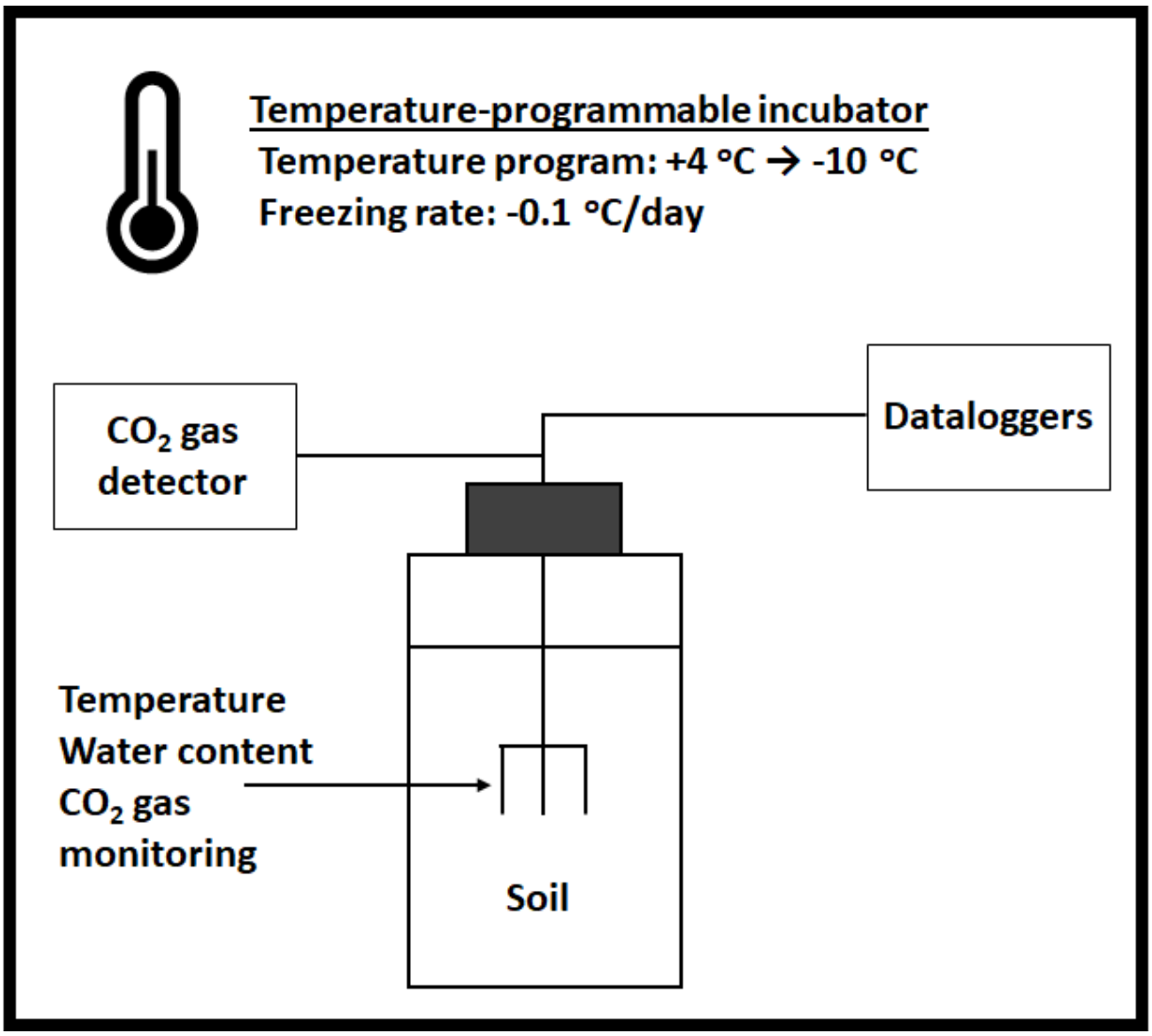
Temperature-programmable incubator
Temperature program: +4 °C → -10 °C
Freezing rate: -0.1 °C/day
CO2 gas detector
Dataloggers
Temperature
Water content
CO2 gas monitoring
Soil

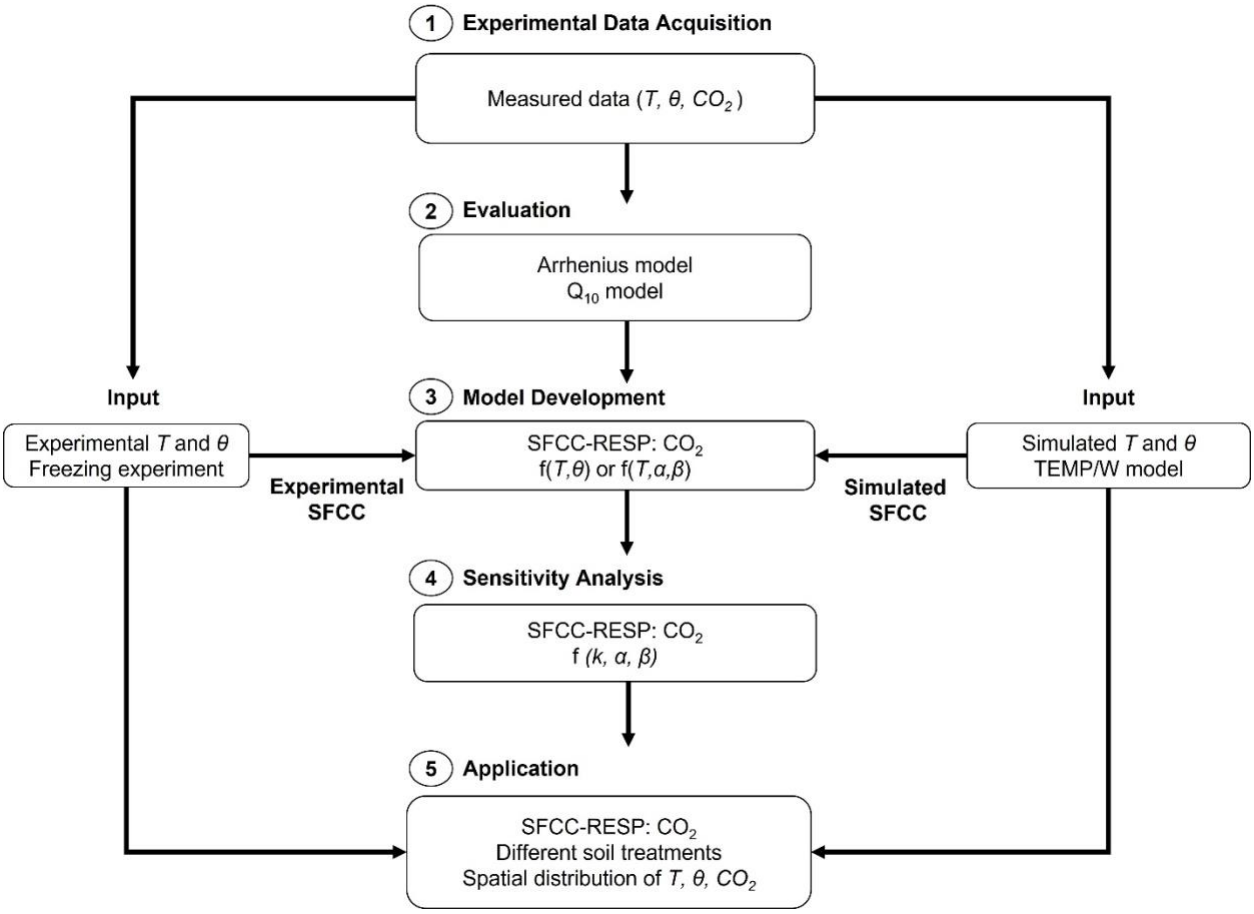
1 Experimental Data Acquisition
Measured data (T, θ, CO2)
2 Evaluation
Arrhenius model
Q10 model
Input
3 Model Development
Input
Experimental T and θ
Freezing experiment
SFCC-RESP: CO2
f(T,θ) or f(T,α,β)
Simulated T and θ
TEMP/W model
Experimental SFCC
Simulated SFCC
4 Sensitivity Analysis
SFCC-RESP: CO2
f (k, α, β)
5 Application
SFCC-RESP: CO2
Different soil treatments
Spatial distribution of T, θ, CO2

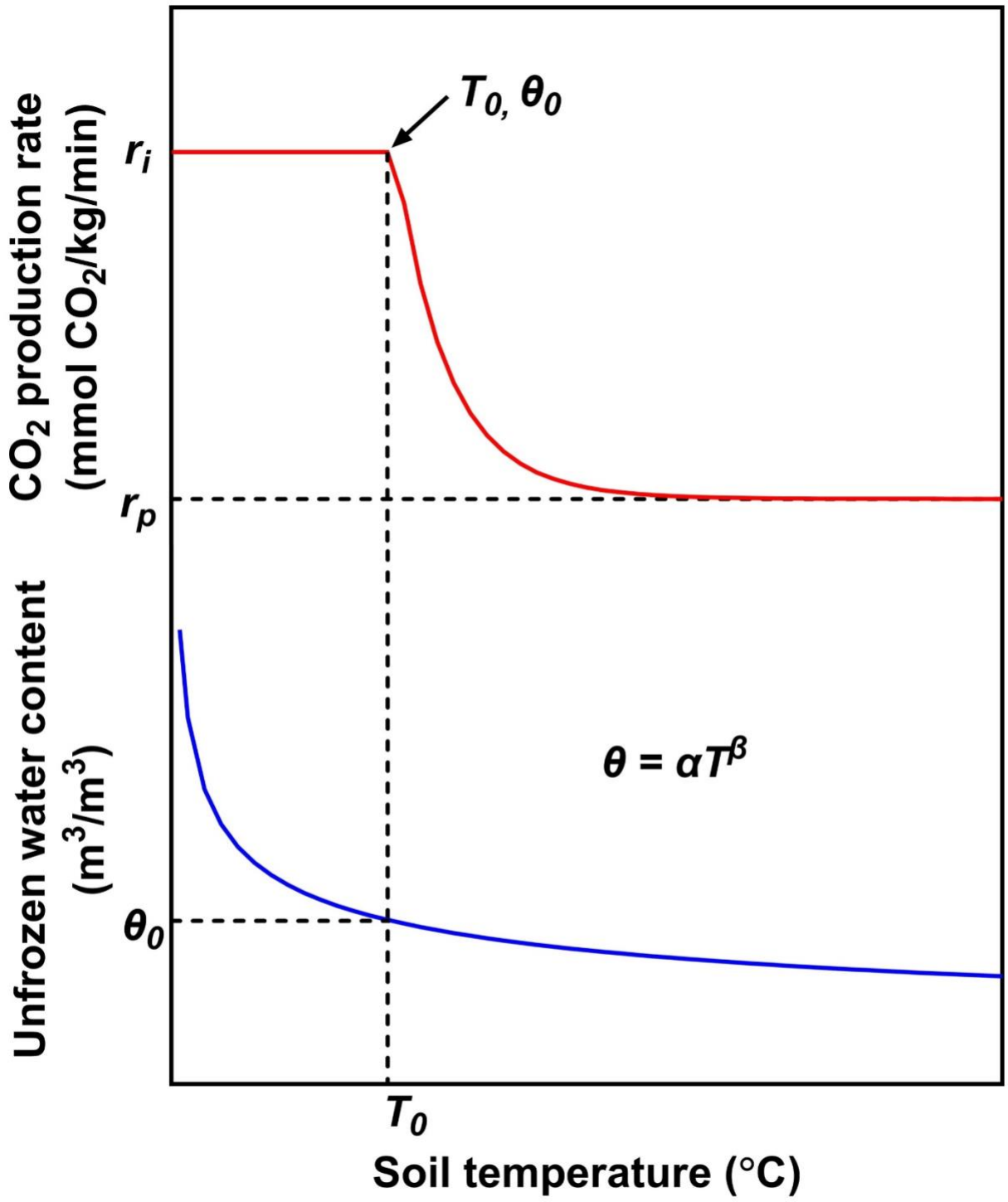
T_0, θ_0
r_i
r_p
CO_2 production rate
(mmol CO_2/kg/min)
Unfrozen water content
(m^3/m^3)
$\theta = \alpha T^{\beta}$
θ_0
T_0
Soil temperature (°C)

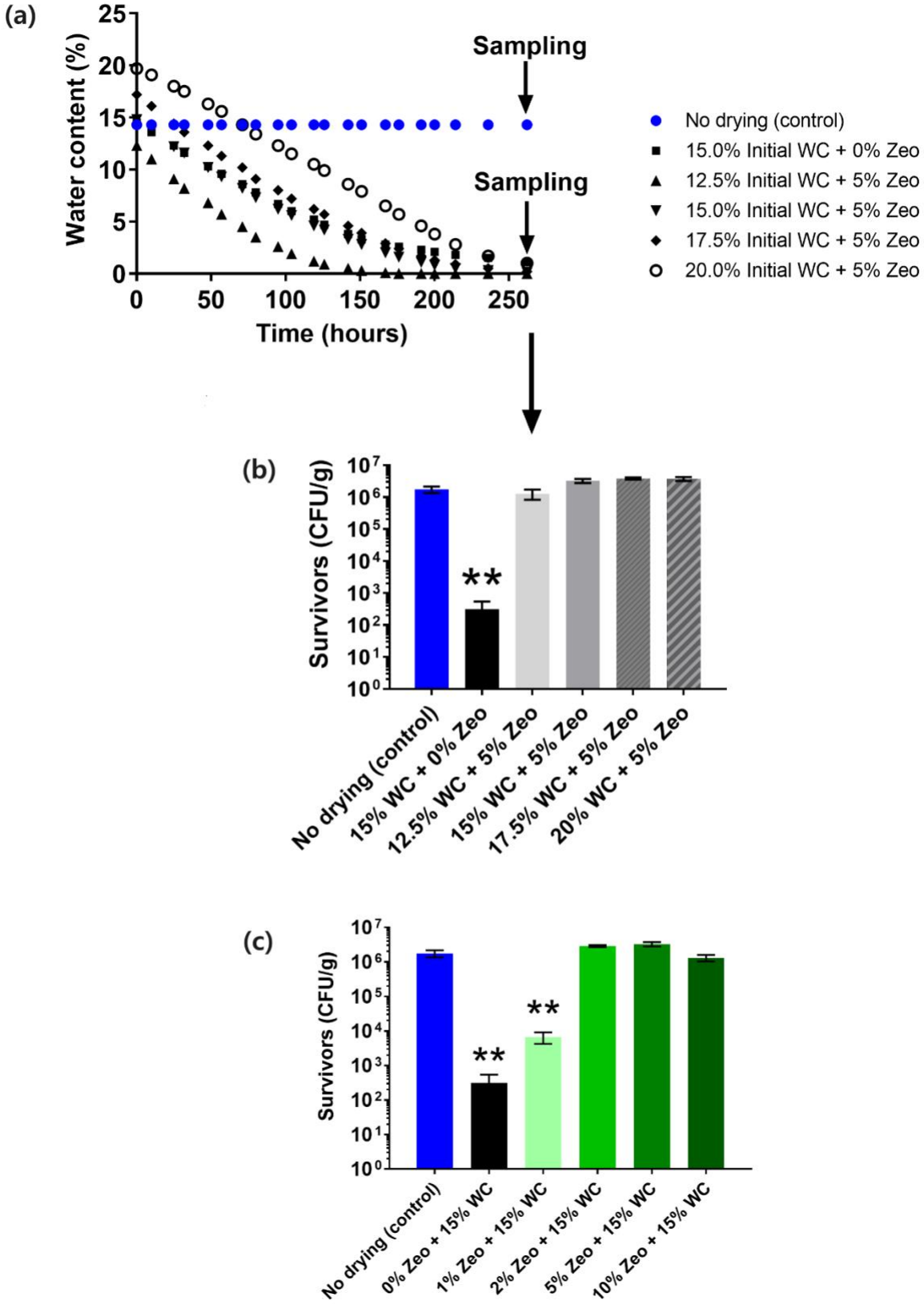
(a)
Water content (%)
Time (hours)
Sampling
Sampling
No drying (control)
15.0% Initial WC + 0% Zeo
12.5% Initial WC + 5% Zeo
15.0% Initial WC + 5% Zeo
17.5% Initial WC + 5% Zeo
20.0% Initial WC + 5% Zeo
(b)
Survivors (CFU/g)
**
No drying (control)
15% WC + 0% Zeo
12.5% WC + 5% Zeo
15% WC + 5% Zeo
17.5% WC + 5% Zeo
20% WC + 5% Zeo
(c)
Survivors (CFU/g)
**
**
No drying (control)
0% Zeo + 15% WC
1% Zeo + 15% WC
2% Zeo + 15% WC
5% Zeo + 15% WC
10% Zeo + 15% WC

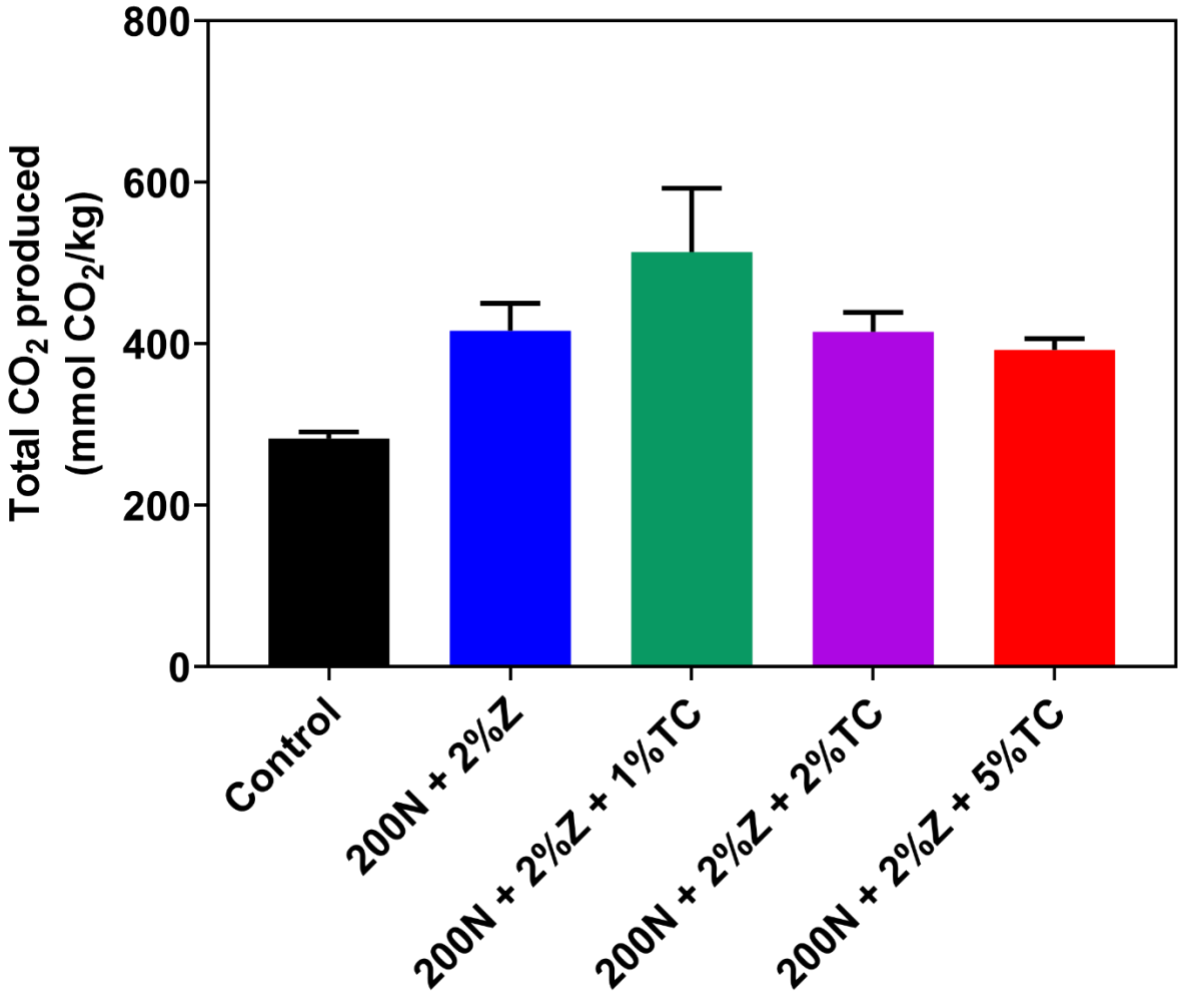
Total CO_2 produced
(mmol CO_2/kg)
800
600
400
200
0
Control
200N + 2%Z
200N + 2%Z + 1%TC
200N + 2%Z + 2%TC
200N + 2%Z + 5%TC

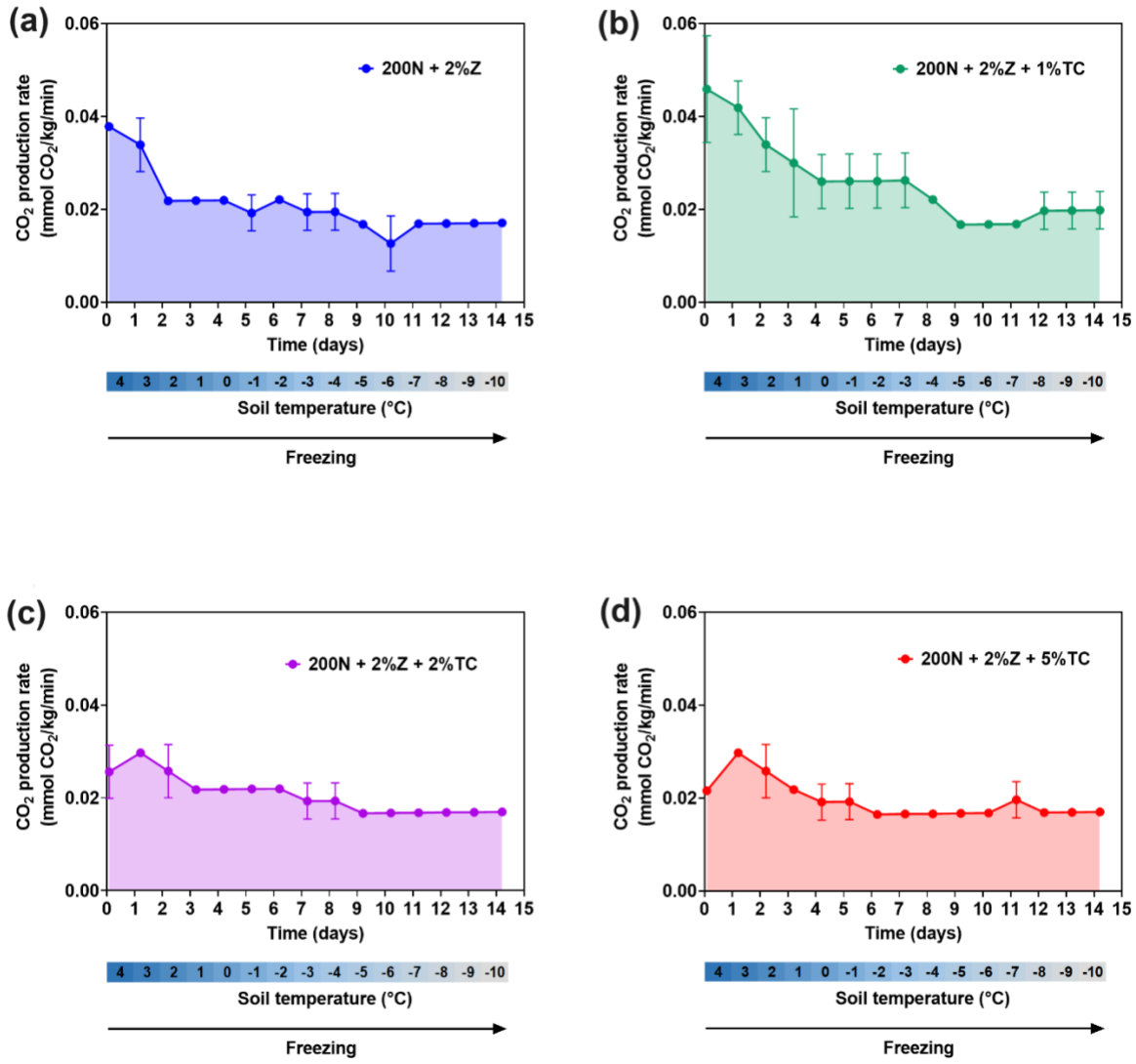
(a)
200N + 2%Z
(b)
200N + 2%Z + 1%TC
(c)
200N + 2%Z + 2%TC
(d)
200N + 2%Z + 5%TC
CO2 production rate (mmol CO2/kg/min)
Time (days)
Soil temperature (°C)
Freezing

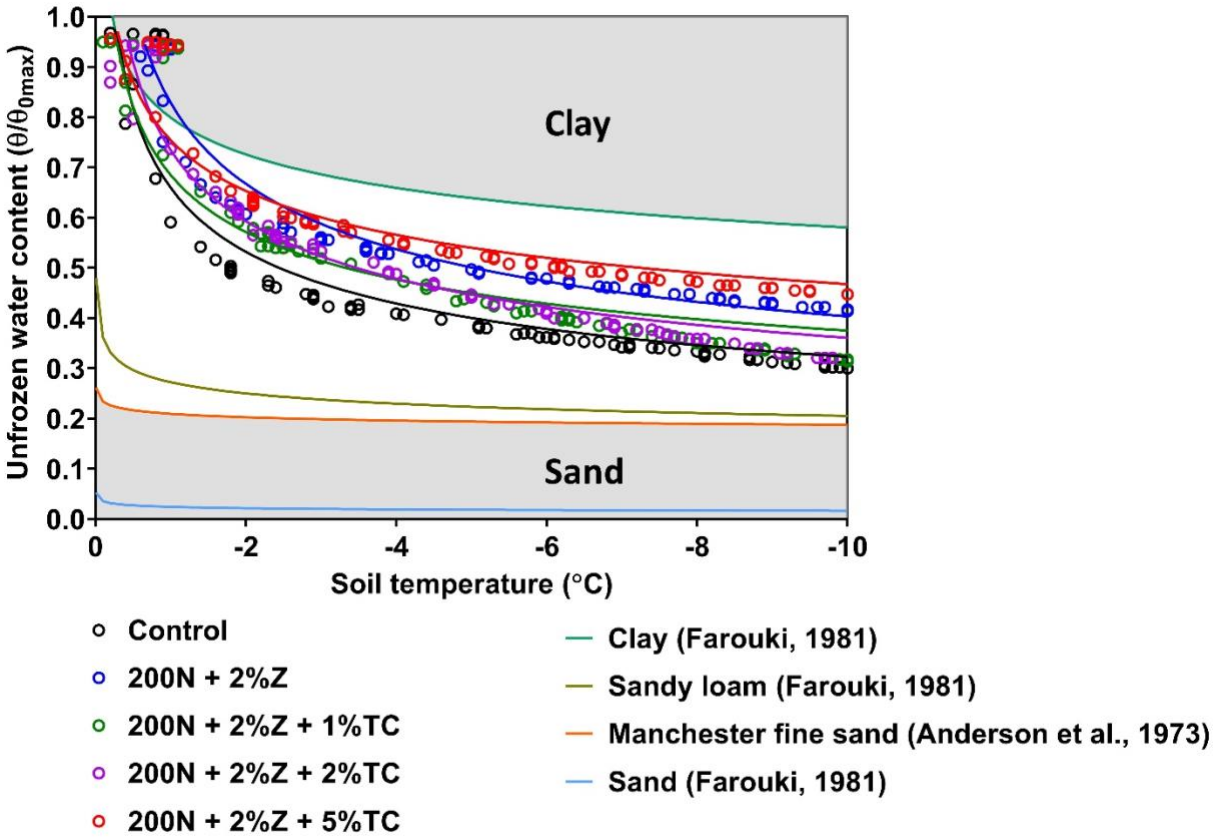
Unfrozen water content (θ/θ0max)
1.0
0.9
0.8
0.7
0.6
0.5
0.4
0.3
0.2
0.1
0.0
Clay
Sand
0
-2
-4
-6
-8
-10
Soil temperature (°C)
Control
200N + 2%Z
200N + 2%Z + 1%TC
200N + 2%Z + 2%TC
200N + 2%Z + 5%TC
Clay (Farouki, 1981)
Sandy loam (Farouki, 1981)
Manchester fine sand (Anderson et al., 1973)
Sand (Farouki, 1981)

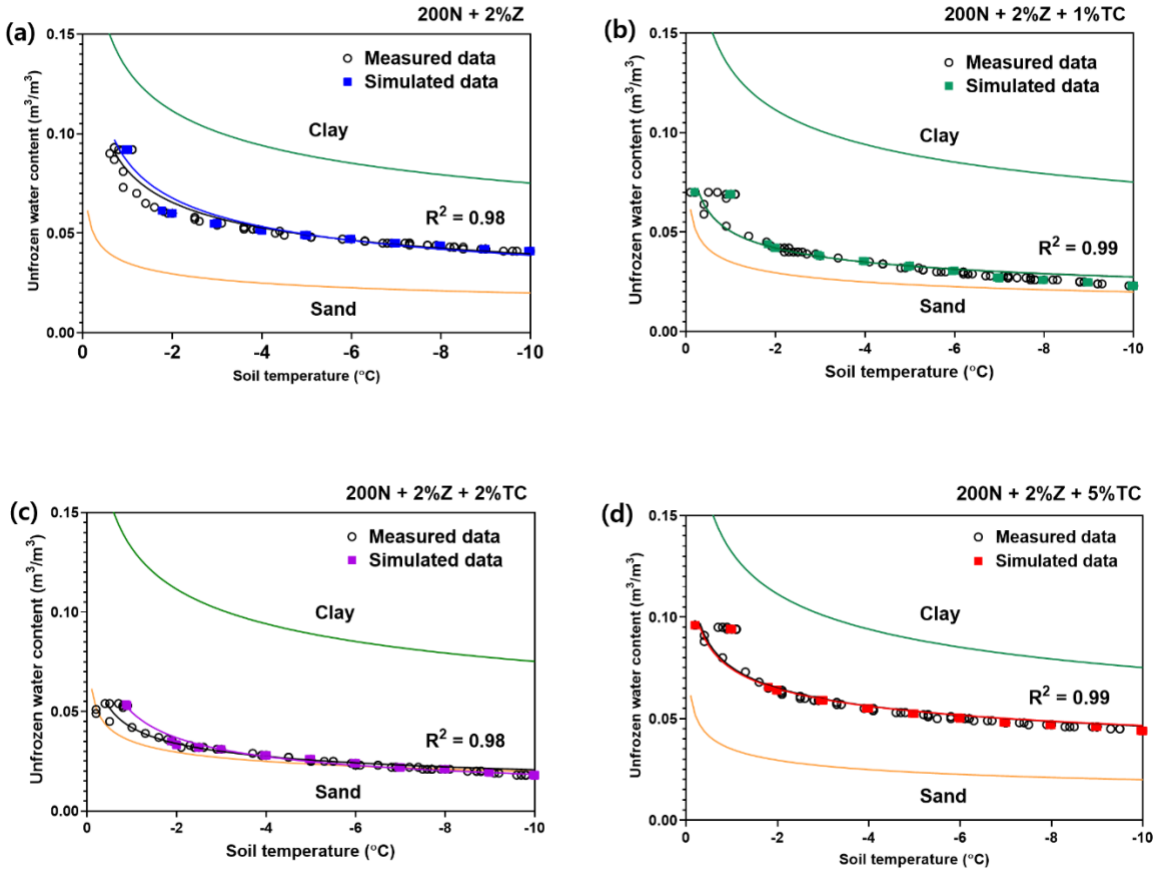
(a)
200N + 2%Z
Measured data
Simulated data
Clay
Sand
R^2 = 0.98
Unfrozen water content (m^3/m^3)
Soil temperature (°C)
(b)
200N + 2%Z + 1%TC
Measured data
Simulated data
Clay
Sand
R^2 = 0.99
Unfrozen water content (m^3/m^3)
Soil temperature (°C)
(c)
200N + 2%Z + 2%TC
Measured data
Simulated data
Clay
Sand
R^2 = 0.98
Unfrozen water content (m^3/m^3)
Soil temperature (°C)
(d)
200N + 2%Z + 5%TC
Measured data
Simulated data
Clay
Sand
R^2 = 0.99
Unfrozen water content (m^3/m^3)
Soil temperature (°C)

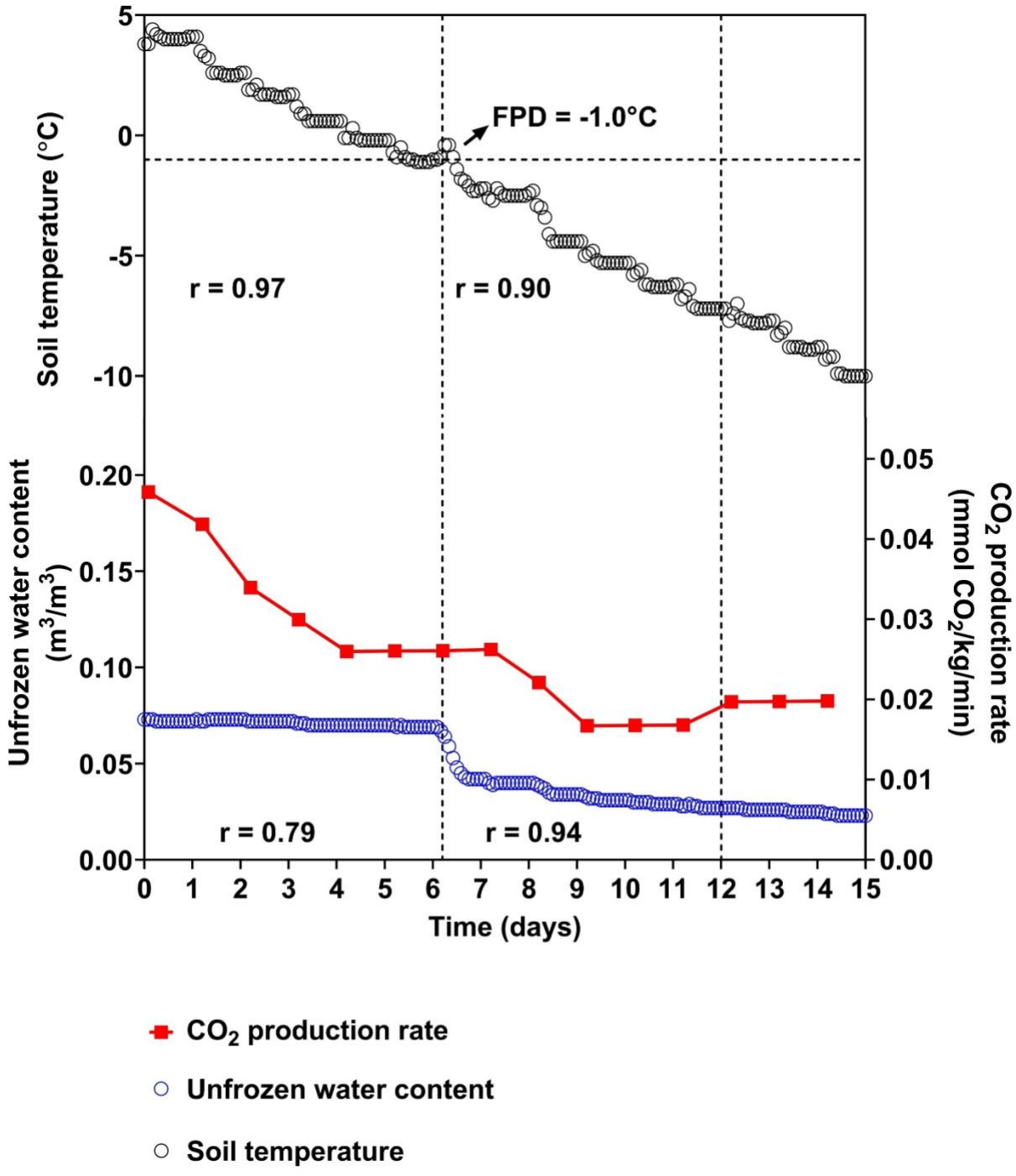
Soil temperature (°C)
Unfrozen water content (m³/m³)
CO₂ production rate (mmol CO₂/kg/min)
Time (days)
FPD = -1.0°C
r = 0.97
r = 0.90
r = 0.79
r = 0.94
CO₂ production rate
Unfrozen water content
Soil temperature

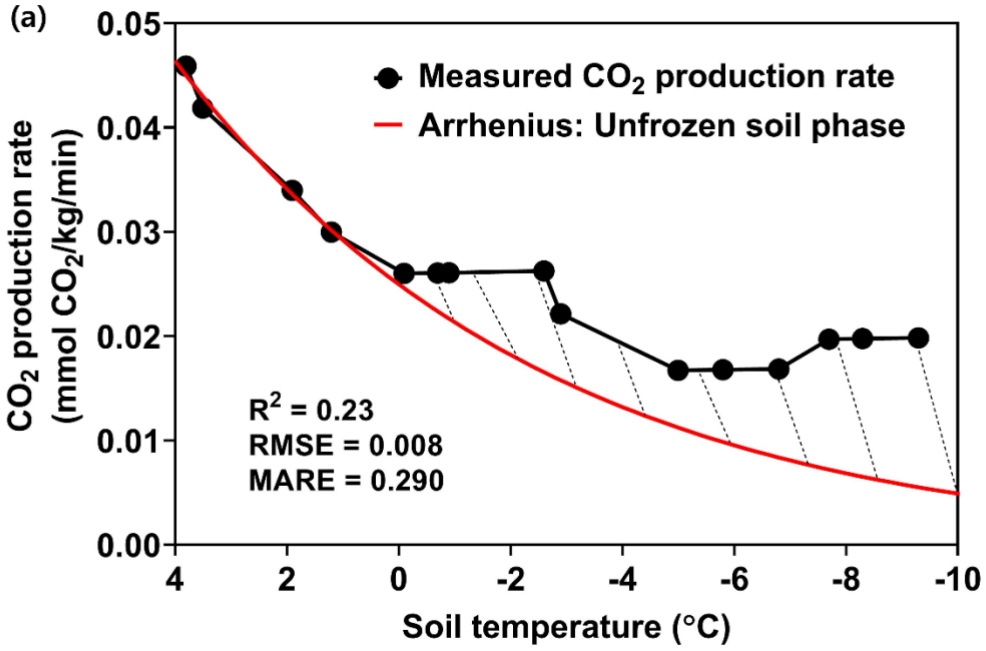
(a)
0.05
0.04
0.03
0.02
0.01
0.00
CO2 production rate
(mmol CO2/kg/min)
Measured CO2 production rate
Arrhenius: Unfrozen soil phase
R2 = 0.23
RMSE = 0.008
MARE = 0.290
4
2
0
-2
-4
-6
-8
-10
Soil temperature (°C)

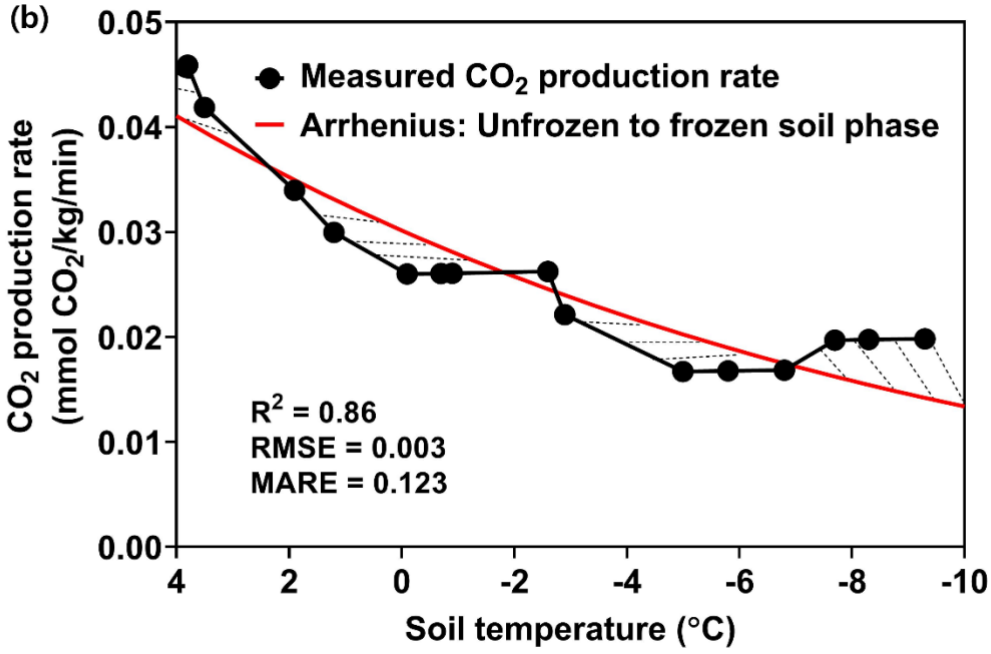
(b)
0.05
0.04
0.03
0.02
0.01
0.00
CO2 production rate
(mmol CO2/kg/min)
Measured CO2 production rate
Arrhenius: Unfrozen to frozen soil phase
R2 = 0.86
RMSE = 0.003
MARE = 0.123
4
2
0
-2
-4
-6
-8
-10
Soil temperature (°C)

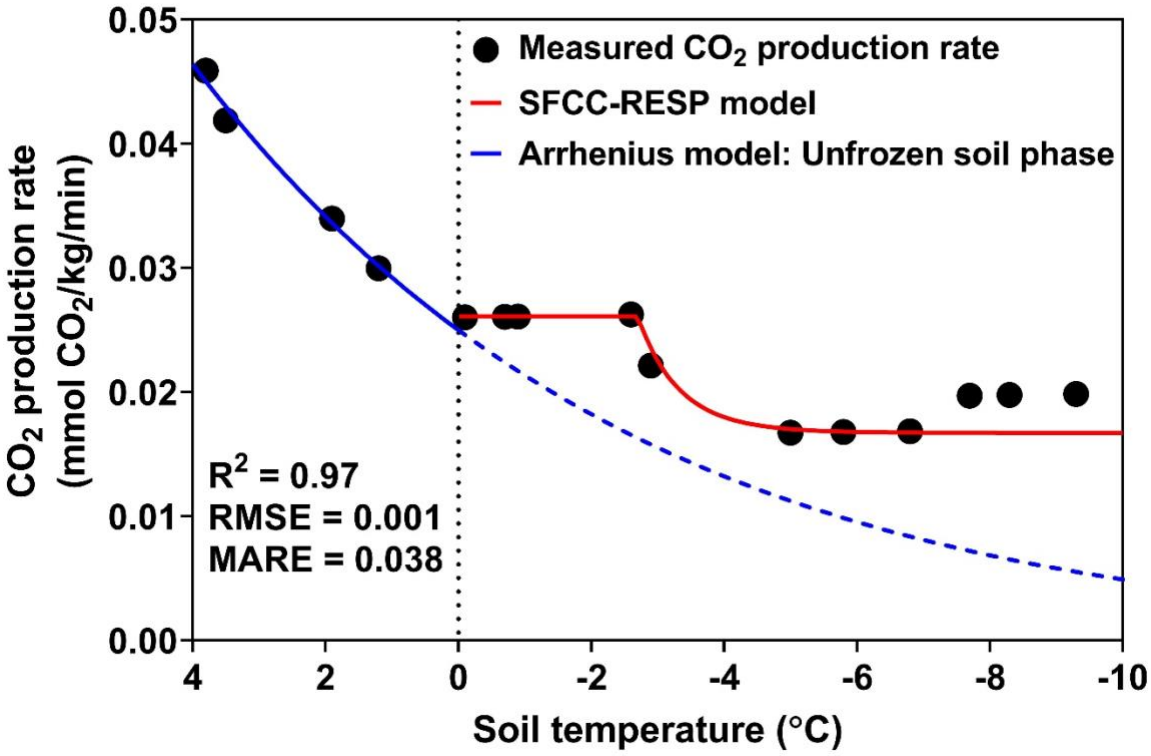
Measured CO_2 production rate
SFCC-RESP model
Arrhenius model: Unfrozen soil phase
R^2 = 0.97
RMSE = 0.001
MARE = 0.038
CO_2 production rate (mmol CO_2/kg/min)
0.05
0.04
0.03
0.02
0.01
0.00
4
2
0
-2
-4
-6
-8
-10
Soil temperature (°C)

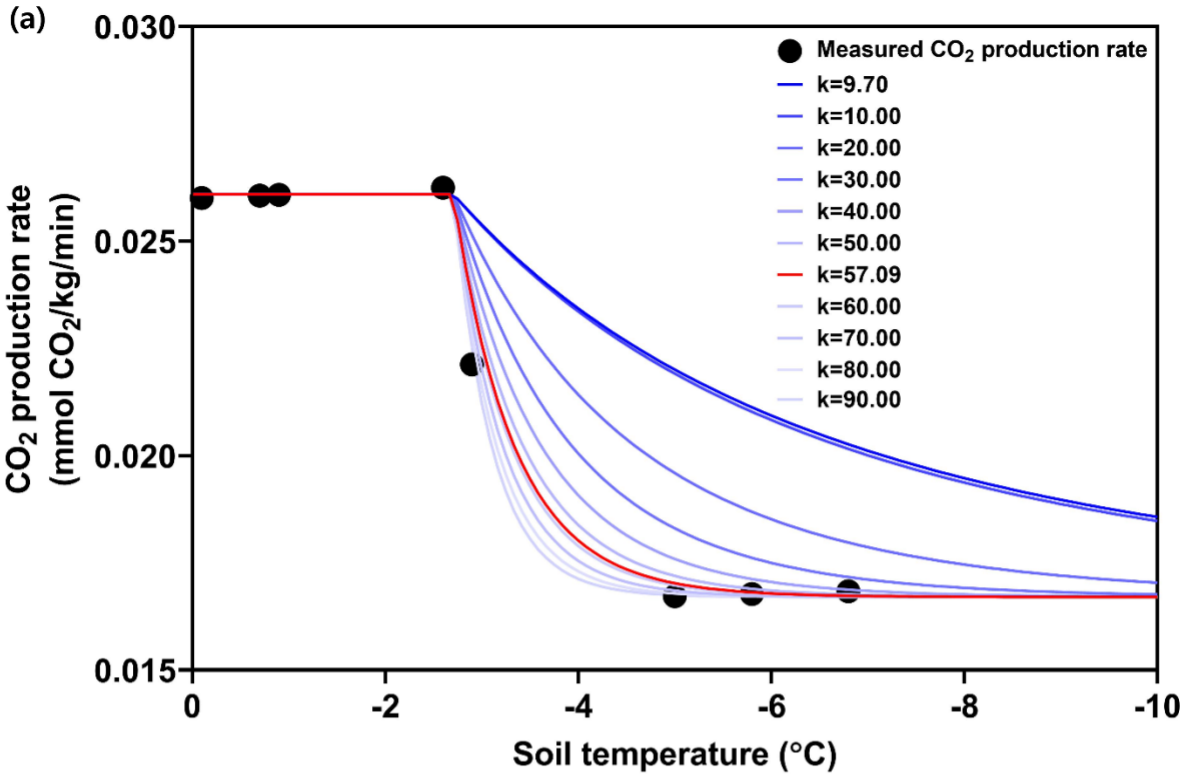
(a)
0.030
0.025
0.020
0.015
CO2 production rate
(mmol CO2/kg/min)
Measured CO2 production rate
k=9.70
k=10.00
k=20.00
k=30.00
k=40.00
k=50.00
k=57.09
k=60.00
k=70.00
k=80.00
k=90.00
0
-2
-4
-6
-8
-10
Soil temperature (°C)

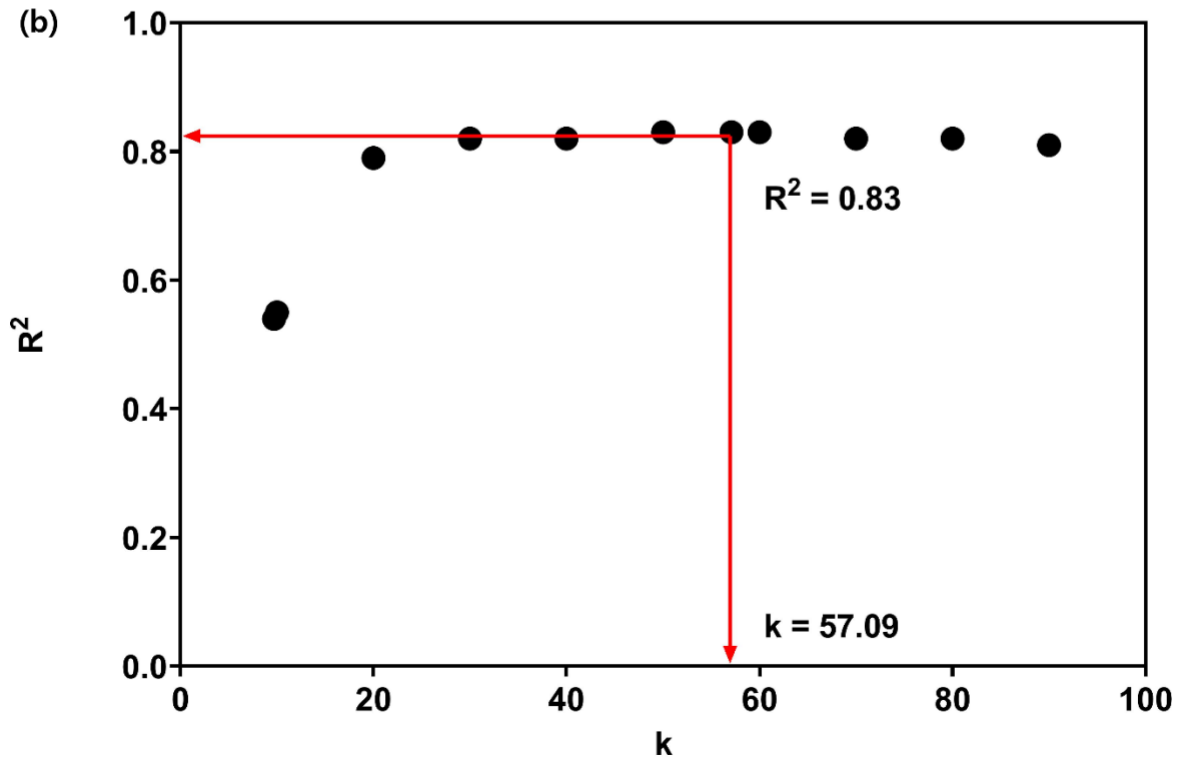
(b)
1.0
0.8
0.6
0.4
0.2
0.0
R2
R2 = 0.83
k = 57.09
0
20
40
60
80
100
k

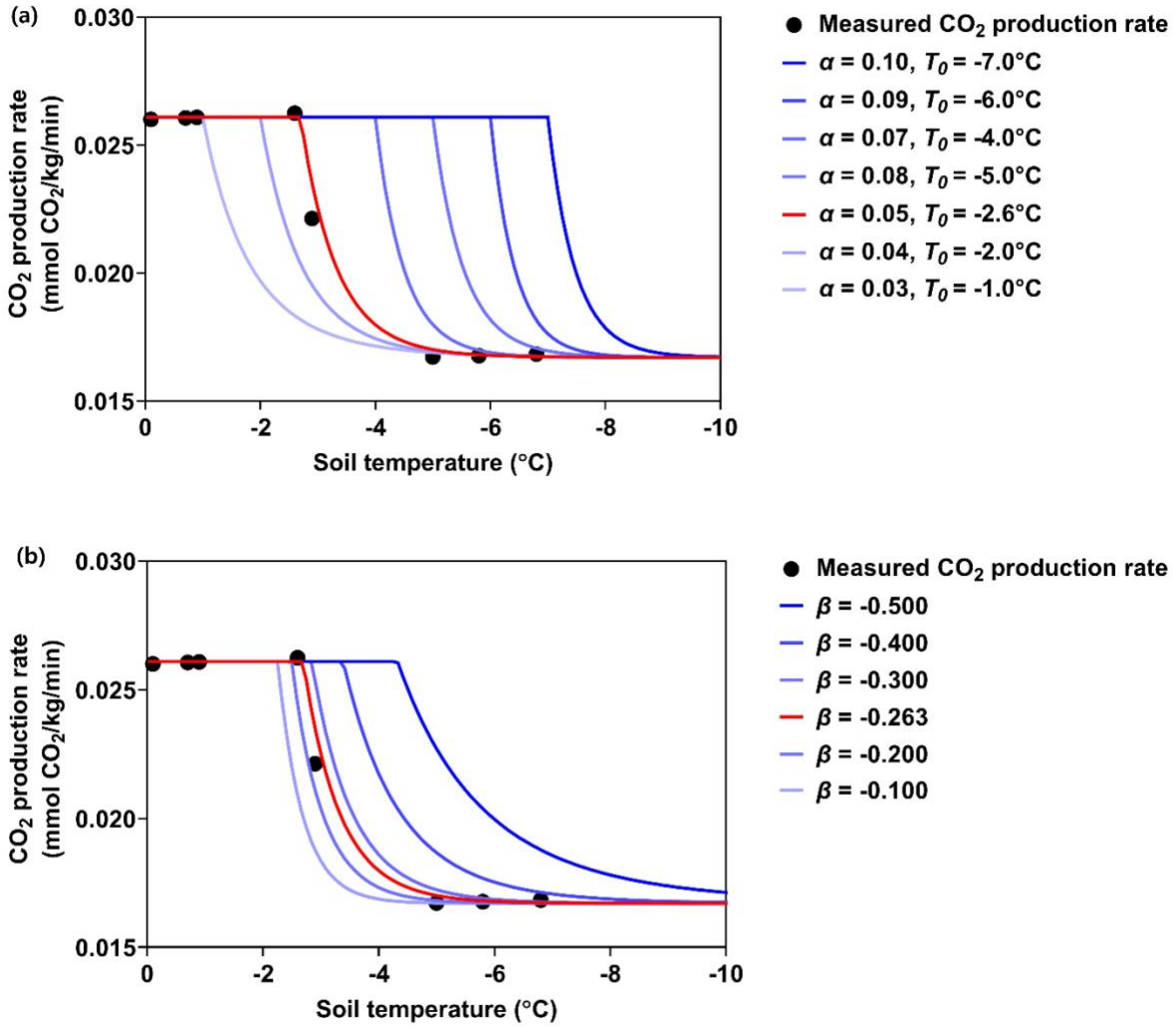
(a)
0.030
0.025
0.020
0.015
CO_2 production rate (mmol CO_2/kg/min)
0
-2
-4
-6
-8
-10
Soil temperature (°C)
Measured CO_2 production rate
α = 0.10, T_0 = -7.0°C
α = 0.09, T_0 = -6.0°C
α = 0.07, T_0 = -4.0°C
α = 0.08, T_0 = -5.0°C
α = 0.05, T_0 = -2.6°C
α = 0.04, T_0 = -2.0°C
α = 0.03, T_0 = -1.0°C
(b)
0.030
0.025
0.020
0.015
CO_2 production rate (mmol CO_2/kg/min)
0
-2
-4
-6
-8
-10
Soil temperature (°C)
Measured CO_2 production rate
β = -0.500
β = -0.400
β = -0.300
β = -0.263
β = -0.200
β = -0.100

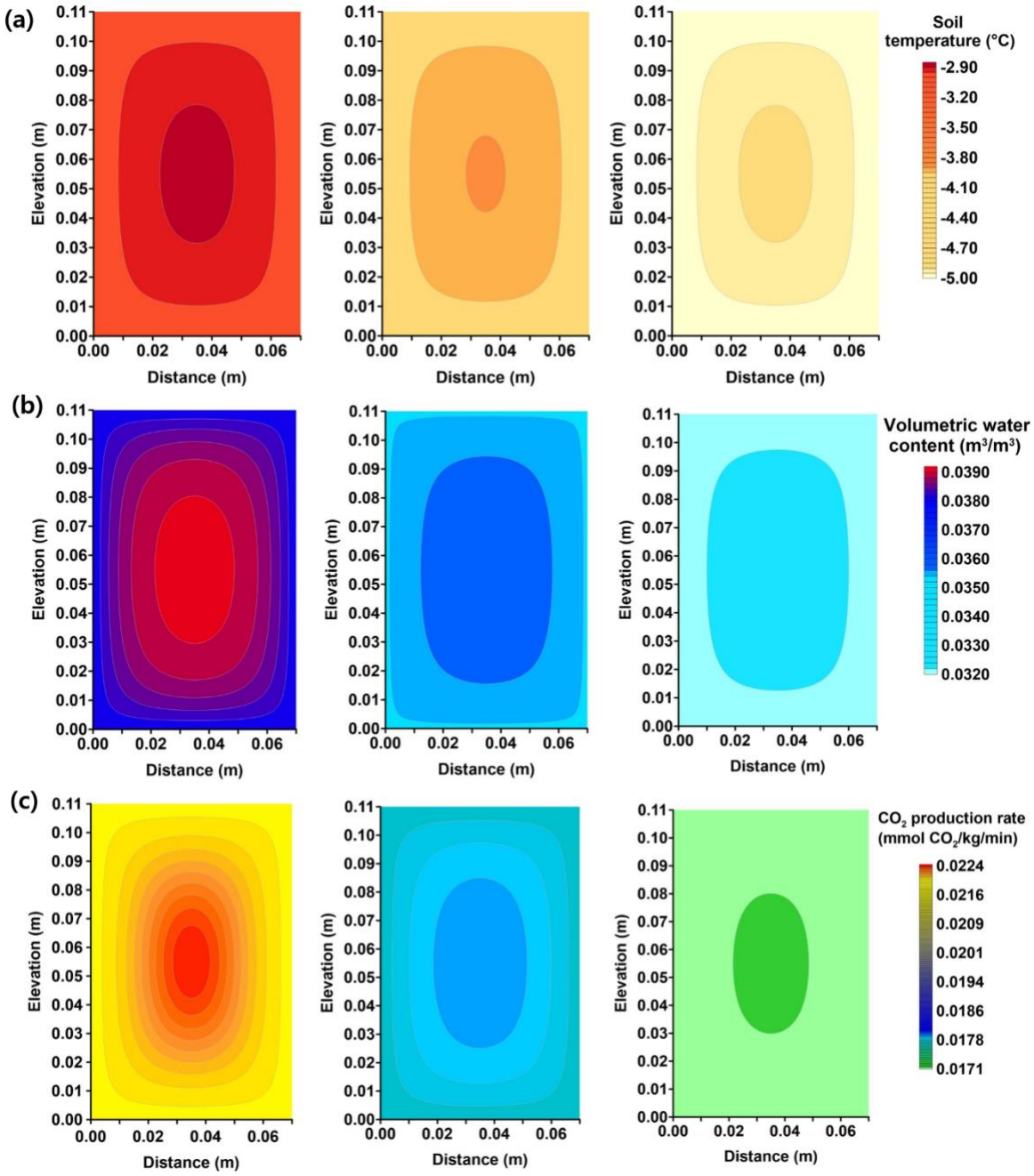
(a)
Elevation (m)
Distance (m)
Soil temperature (°C)
-2.90
-3.20
-3.50
-3.80
-4.10
-4.40
-4.70
-5.00
(b)
Volumetric water content (m³/m³)
0.0390
0.0380
0.0370
0.0360
0.0350
0.0340
0.0330
0.0320
(c)
CO2 production rate (mmol CO2/kg/min)
0.0224
0.0216
0.0209
0.0201
0.0194
0.0186
0.0178
0.0171

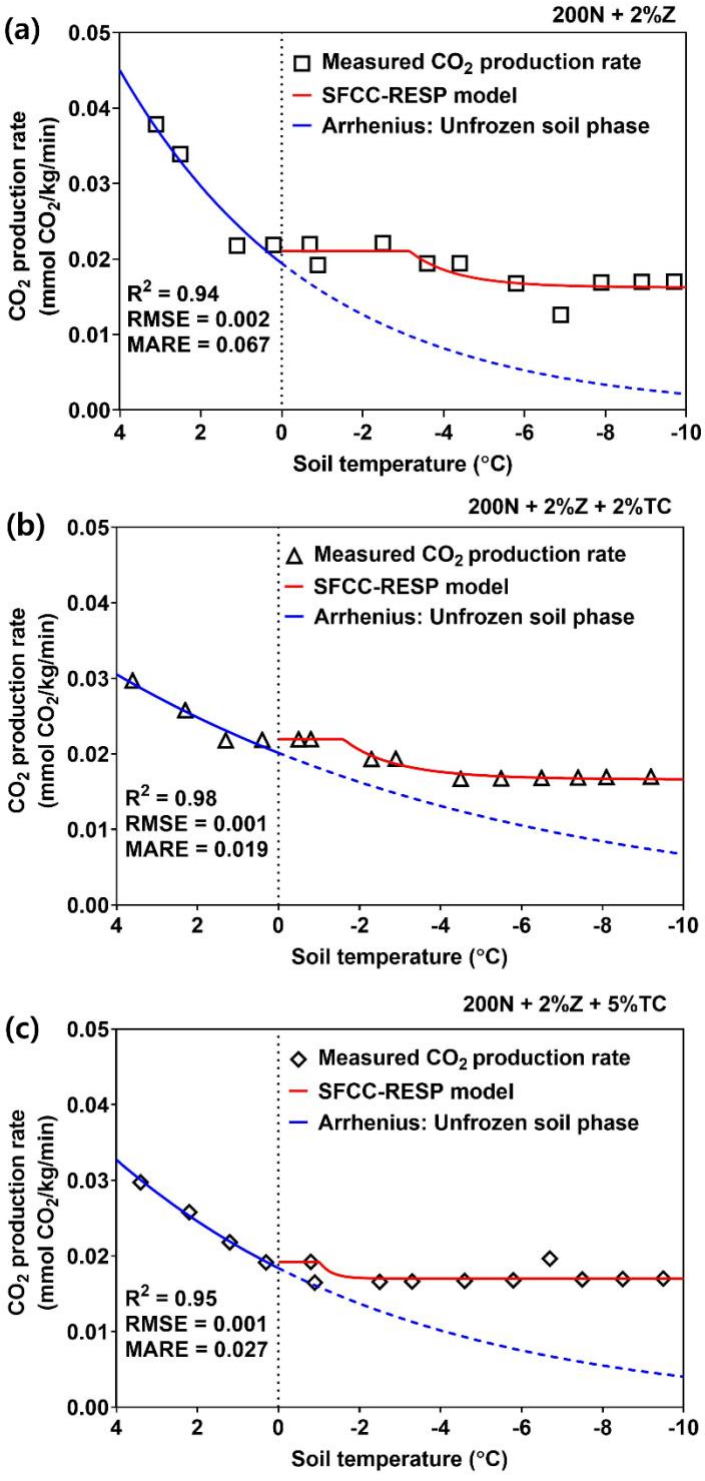
(a)
200N + 2%Z
Measured CO_2 production rate
SFCC-RESP model
Arrhenius: Unfrozen soil phase
R^2 = 0.94
RMSE = 0.002
MARE = 0.067
CO_2 production rate (mmol CO_2/kg/min)
Soil temperature (°C)
(b)
200N + 2%Z + 2%TC
Measured CO_2 production rate
SFCC-RESP model
Arrhenius: Unfrozen soil phase
R^2 = 0.98
RMSE = 0.001
MARE = 0.019
CO_2 production rate (mmol CO_2/kg/min)
Soil temperature (°C)
(c)
200N + 2%Z + 5%TC
Measured CO_2 production rate
SFCC-RESP model
Arrhenius: Unfrozen soil phase
R^2 = 0.95
RMSE = 0.001
MARE = 0.027
CO_2 production rate (mmol CO_2/kg/min)
Soil temperature (°C)

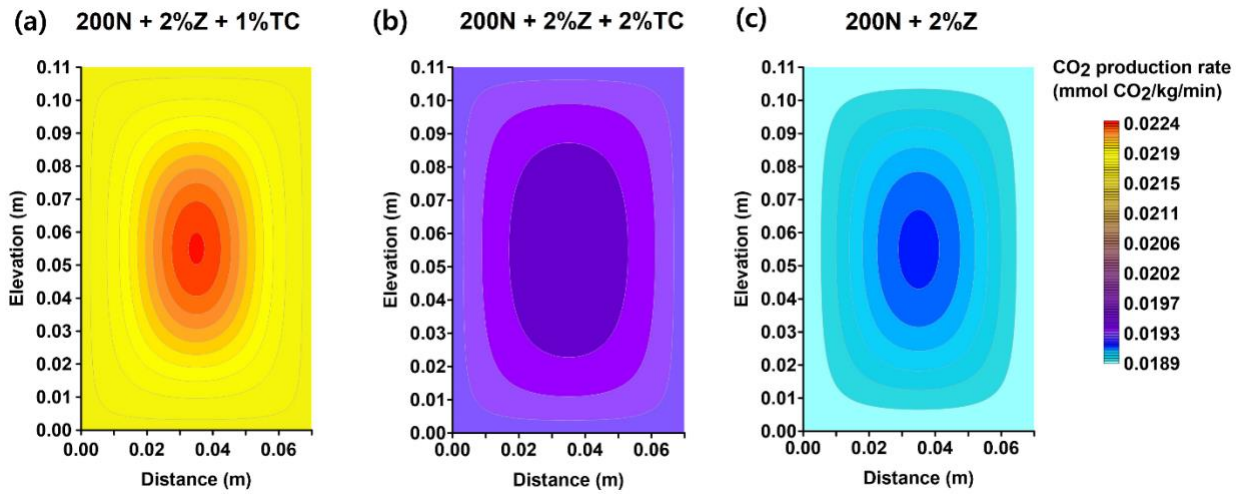
(a) 200N + 2%Z + 1%TC
(b) 200N + 2%Z + 2%TC
(c) 200N + 2%Z
Elevation (m)
Distance (m)
0.00
0.01
0.02
0.03
0.04
0.05
0.06
0.07
0.08
0.09
0.10
0.11
0.00
0.02
0.04
0.06
CO2 production rate
(mmol CO2/kg/min)
0.0224
0.0219
0.0215
0.0211
0.0206
0.0202
0.0197
0.0193
0.0189

Table 1 Summary of the physical, chemical, and microbial characteristics of the cold-climate soil contaminated with petroleum hydrocarbons

	Properties	Unit	Value
Physical	USCS-based classification[1]	-	Poorly graded sand with gravel
	USDA-based classification[2]	-	Sandy loam
	Gravimetric water content	%	11.6
Chemical	Ammonia as nitrogen	mg/kg	< 5
	Nitrate as nitrogen	mg/kg	10
	Nitrite as nitrogen	mg/kg	< 5
	Total Kjeldahl nitrogen	mg/kg	240
	Phosphorus	mg/kg	380
	Potassium	mg/kg	4500
	Sodium	mg/kg	450
	Cation exchange capacity (CEC)	meq/100 g	20
	Organic carbon	%	0.53
	CCME PHC-F2 (C10-C16)[3]	mg/kg	0-2000
	CCME PHC-F3 (C16-C34)[4]	mg/kg	1200-9000
	Soil pH	-	7.62
Microbial	Viable heterotrophs[5]		
	4 °C	CFU/g	2.4×10^6
	15 °C	CFU/g	2.0×10^7
	22 °C	CFU/g	4.3×10^7
	Viable diesel-degrading bacteria[6]		
	4 °C	CFU/g	2.5×10^4
	15 °C	CFU/g	3.8×10^6
	22 °C	CFU/g	2.2×10^7

[1]USCS (Unified Soil Classification System): 9% gravel, 5% coarse sand, 14% medium sand, 44% fine sand, 16% silt, 11% clay. $C_u = 3.85$ and $C_c = 1.04$.
[2]USDA (United States Department of Agriculture): 68% sand, 19% silt, 13% clay.
[3,4]CCME (Canadian Council of Ministers of the Environment) petroleum hydrocarbon fractions.
[5]Viable heterotroph counting using R2A (Reasoner's 2A agar).
[6]Viable diesel degraders using Bushnell Hass agar spiked with 0.5% diesel.

Table 2. Correlation analyses for CO_2 production (mmol/kg/min) with soil temperature and unfrozen water content, performed separately for temperatures above and below the depressed freezing points of the treated soils.

		Temperature effect		Unfrozen water content effect	
Soil phase	Soil treatment	[1]Correlation r	[2]Significance	[1]Correlation r	[2]Significance
Unfrozen phase[3]	200N + 2%Z	**0.93**	**	0.65	ns
	200N + 2%Z + 1%TC	**0.97**	***	**0.79**	*
	200N + 2%Z + 2%TC	**0.83**	*	0.70	ns
	200N + 2%Z + 5%TC	**0.75**	ns	0.64	ns
Freezing phase[4]	200N + 2%Z	**0.82**	*	**0.83**	*
	200N + 2%Z + 1%TC	**0.90**	*	**0.94**	*
	200N + 2%Z + 2%TC	**0.89**	*	**0.93**	*
	200N + 2%Z + 5%TC	-	-	-	-

[1]Pearson's correlation coefficient. [2]Significance: *: $p<0.05$, **: $p<0.01$, ***: $p<0.001$, ns: not significant.

[3]Unfrozen phase: from 4 to −1 °C (freezing point of each treated soil)

[4]Freezing phase: −1 to −8 °C.

Table 3. Mathematical equations of the developed SFCC-RESP model which integrates the Arrhenius and RESP models to account for the emerging effect of unfrozen water below 0 °C on soil respiration activity.

Temperature regime	Model	Equation	Influencing factors
$T > 0$ °C	Arrhenius model	$RESP = Ae^{-\frac{Ea}{RT}}$	Temperature
$T < 0$ °C	SFCC-RESP	$T_o < T < 0$°C: $RESP = r_i$; $T < T_o$: $RESP = r_p + (r_i - r_p)e^{-k\alpha(T^{(\beta+1)} - T_o^{(\beta+1)})}$	Temperature and unfrozen water

Arrhenius equation described in Section 2.4.2

T_o, r_i, and r_p described in Figure 3